People's Democratic Republic of Algeria
Ministry of Higher Education and Scientific Research
University of Echahid Hamma Lakhdar - El Oued

Faculty of Technology

Department of Electrical Engineering

A Master's Thesis presented to obtain the diploma of

Academic Master in Electrical Engineering

Discipline: Science and Technology

Specialty: Electric control

Control of Induction Motor based on the Classical and Advanced Techniques

Presented and defended by:

Douis Ammar

Zaiz Mousab

Zelaci Hammoudi

Under jury members:

Chouaib LABIOD	**Examiner**	A. Professor at the University of El Oued
Hakima CHERIFA	**Examiner**	A. Professor at the University of El Oued
Zoheir TIR	**Supervisor**	Professor at the University of El Oued

Academic Year: 2022/2023

Dedication

First and foremost, we would like to express our profound gratitude to the Almighty Allah for graciously endowing us with the strength and patience necessary to successfully accomplish this endeavor.

We wish to convey our heartfelt dedication to the extraordinary individuals who have played a pivotal role in enabling us to attain our objective.

To our beloved parents, whose unwavering love, steadfast support, and unwavering faith in our abilities have served as an enduring source of inspiration.

To our esteemed supervisor, whose invaluable guidance, unwavering encouragement, and approachability have been instrumental in our triumph.

We would also like to extend our sincere appreciation to our extended family members and close friends for their steadfast support and unwavering encouragement.

Lastly, we would like to express our deepest gratitude to all our esteemed professors for their invaluable mentorship, unwavering guidance, and profound knowledge imparted throughout our academic journey.

Acknowledgments

We couldn't have done this research without the help of many people, although we can't mention their names here. We want to thank our supervisor, Mr. Zoheir TIR, for his constant help and useful advice. We also appreciate the administrative team for their support. We're grateful to our teachers for their guidance. We also want to acknowledge the LEVRES laboratory for hosting us and providing resources. Their support was crucial in completing this project successfully. However, any mistakes or oversights in this dissertation are our responsibility.

Contents:

List of Figures

Summary

Nonlinear systems play a significant role in industrial applications, and among them, the induction motor stands out for its exceptional performance when compared to other types of motors. Consequently, there is a growing interest in developing nonlinear control methods to further improve its performance. The initial part of this thesis focuses on two distinct control techniques: vector control with rotor flux orientation and scalar control. These approaches aim to achieve dynamic performance by utilizing proportional-integral (PI) controllers. In the following section, a new nonlinear control approach based on Backstepping is introduced. This approach effectively enhances the dynamic performance of the motor by leveraging the principles of Lyapunov theory. Throughout this research, comprehensive simulation results are presented, along with various insightful observations.

Keywords: Induction motor (IM), Vector control, Scalar control, Lyapunov theory, Backstepping control.

الملخص

الأنظمة غير الخطية تلعب دورًا هامًا في التطبيقات الصناعية، ومن بينها، تبرز محرك الحث لأدائه الاستثنائي مقارنةً بأنواع أخرى من المحركات. ونتيجة لذلك، هناك اهتمام متزايد في تطوير قوانين التحكم غير الخطية لتعزيز أدائه بشكل أكبر. يركز الجزء الأول من هذه الأطروحة على تقنيتي التحكم المتجهي مع توجيه مجال الدوران والتحكم العلمي. الهدف الرئيسي لهذه النهجين هو تحقيق أداء ديناميكي باستخدام وحدات تحكم نسبية-تكاملية (PI). في الجزء التالي، يتم تقديم نهج تحكم غير خطي جديد يستند إلى تقنية الباكستيبنغ باستخدام نظرية ليابونوف لتعزيز الأداء الديناميكي للمحرك بفعالية. تشمل هذه الأطروحة عرضًا شاملاً لجميع نتائج المحاكاة التي تم الحصول عليها طوال هذا البحث، مصحوبة بملاحظات مفيدة متنوعة.

كلمات مفتاحية: المحرك الحثي، التحكم الشعاعي، التحكم السلمي، تقنية التحكم الباكستيبنغ ، نظرية ليابينوف.

General Introduction

In the domain of industrial applications, direct current (DC) motors have gained widespread utilization due to their straightforward structures, enabling easy control of flux and torque based on current levels. Nonetheless, the maintenance expenses and energy consumption associated with the rotating components of DC motors have directed researchers' attention toward alternating current (AC) motors, particularly synchronous and asynchronous motors [1]. The induction motor, renowned for its uncomplicated design, low maintenance requirements, satisfactory performance, and cost-effectiveness, has emerged as the most commonly employed electric motor in various industries. Nevertheless, this simplicity is accompanied by physical complexity arising from the electromagnetic interactions among its constituents and the non-linear mathematical model. Efficiently controlling the induction motor for variable speed drives presents a challenge as not all variables can be directly measured, and parameters may exhibit variation during operation [2].

In contrast to DC motors that can adjust speed by altering the voltage, induction motors necessitate variable frequency AC currents. One major impediment has been the inverter, which impedes precise control of the motor-inverter system dynamics [1]. Consequently, the induction motor has predominantly been employed at constant speeds, limiting its applicability in scenarios requiring variable speed operation. However, advancements in power electronics and digital electronics have facilitated the development of real-time control techniques that enable effective regulation of flux and torque, thereby facilitating variable speed control [2].

To achieve variable speed operation in the induction motor, an external process must regulate the supply voltage. Various control methods have been employed, including vector control, which can achieve performance comparable to that of DC motors [3]. Although vector control remains effective under changing conditions, accurate knowledge of motor parameters is crucial as control dynamics depend on them. Conventional control methods utilizing proportional-integral (PI) controllers, while still prevalent, may prove insufficient [3]. Therefore, state feedback control laws have been devised. This study proposes the utilization of the Backstepping technique, a recursive control method for studying dynamic stability, in conjunction with field-oriented control, a recent technique for nonlinear systems. The control laws are designed based on the principle of field-oriented control with rotor flux orientation. Initially, the state variables required for controlling the induction motor are assumed to be measured by sensors and subsequently estimated using various algorithms [4].

The thesis follows the following structure: The first chapter presents the mathematical model of the induction motor based on simplifying assumptions and the Park transformation. The second chapter introduces the principles of scalar control and vector control using PI-type controllers. Subsequently, simulations and analysis of the results under different motor operating conditions are conducted. The third chapter focuses on the theoretical exposition of the Backstepping technique and its application to the induction motor in combination with direct field-oriented control with rotor flux orientation. Simulation results demonstrating the robustness of the control technique under various operating conditions are presented. Finally, the conclusion summarizes the main findings of the study.

In the field of industrial applications, direct current (DC) motors have been widely used due to their simple structures, which allow for easy control of flux and torque based on current. However, the maintenance costs and energy consumption associated with the rotating parts of DC motors have led researchers to focus on alternating current (AC) motors, specifically synchronous and asynchronous motors [1]. The induction motor, known for its simple design, ease of maintenance, performance, and affordability, has become the most commonly used electric motor in the industry. However, this simplicity comes with physical complexity due to the electromagnetic interactions between its components and the non-linear mathematical model. Controlling the induction motor for variable speed drives is a challenge as not all variables can be directly measured, and parameters may vary during operation [2].

Unlike DC motors, which can adjust speed by changing the voltage, induction motors require variable frequency AC currents. One major obstacle has been the inverter, which hinders precise control of the motor-inverter system dynamics [1]. As a result, the induction motor has primarily been used at constant speeds, limiting its application in scenarios that require variable speed operation. However, advancements in power electronics and digital electronics have enabled the development of real-time control techniques that allow effective regulation of flux and torque, facilitating variable speed control [2].

To achieve variable speed operation in the induction motor, an external process must control the supply voltage. Various control methods have been applied, including vector control, which can achieve performance comparable to that of DC motors [3]. Vector control remains effective during changing conditions, but accurate knowledge of motor parameters is crucial as control dynamics depend on them. Conventional control methods using proportional-integral (PI) controllers, while still commonly used, may be insufficient [3]. Therefore, state feedback control laws have been developed. In this study, the Backstepping technique, a recursive control method for studying dynamic stability, is proposed in combination with field-oriented control, a recent technique for nonlinear systems. The control laws are designed based on the principle of field-oriented control with rotor flux orientation. Initially, the state variables required for controlling the induction motor are assumed to be measured by sensors and later estimated using various algorithms[4].

The structure of the thesis is as follows: The first chapter presents the mathematical model of the induction motor based on simplifying assumptions and the Park transformation. The second chapter introduces the principles of scalar control and vector control using PI-type controllers. Simulation and analysis of the results under different motor operating conditions are then performed. The third chapter focuses on the theoretical presentation of the Backstepping technique and applies it to the induction motor in combination with direct field-oriented control with rotor flux orientation. Simulation results demonstrating the robustness of the control technique under various operating conditions are presented. Finally, the conclusion summarizes the main findings of the study.

Chapter 1

Modeling of the Induction Machine

1.1 Introduction

The induction motor (IM) is the most commonly used machine in over 80% of applications. It can be found in various applications today, including transportation (metros, trains, and ship propulsion), industrial settings (such as machine tools), and household appliances. This motor is preferred due to its primary benefit, which is its simple and sturdy structure that is easy to construct, made possible by the absence of sliding electrical contacts. It is used in a wide range of power applications, from just a few watts to several megawatts [2].

This chapter aims to introduce the modeling principle of the IM. The first section will focus on modeling the IM, which involves establishing a mathematical model for the specific machine being studied. The second section will involve transforming the three-phase system into a two-phase system using Park's transformation.

1.2. Modeling of the IM

In order to simulate and control the operation of the IM (Induction Motor) during changing conditions, it is necessary to have a model of the machine. This chapter provides an overview of the key steps and results involved in the modeling process, which will be discussed in greater detail later on. The specific IM being examined in our study is depicted in Figure (1.1).

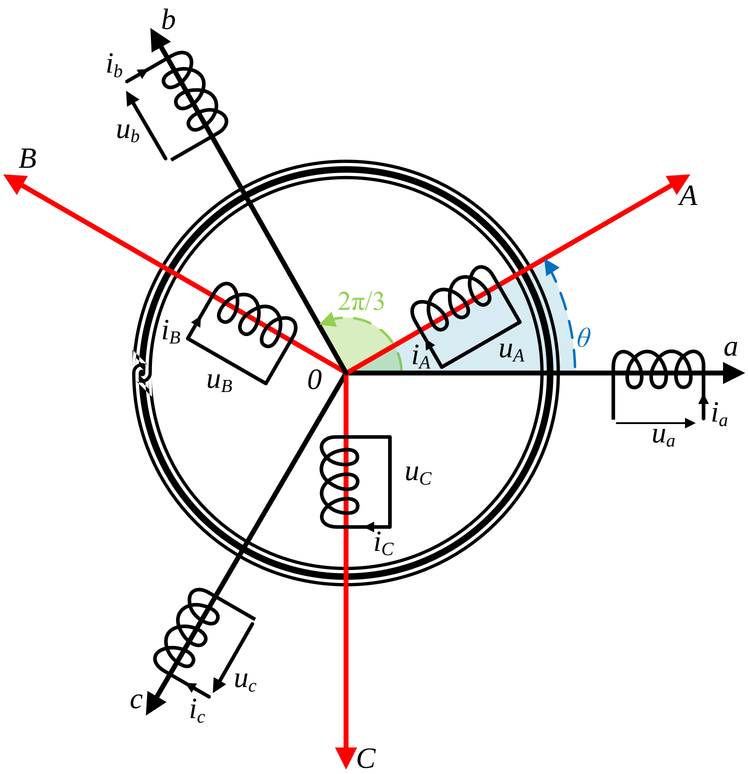

Figure 1.1 Representation of the stator and rotor windings of an induction motor (IM).

The stator of an electric motor consists of a ring of laminations with notches inside; carrying a three-phase winding that resembles an alternator. This winding is typically connected to the power source and serves as the primary winding.

On the other hand, the rotor is another ring of laminations, grooved on the outside, and positioned concentrically with the stator. The rotor is separated from the stator by a narrow and constant air gap. It contains a short-circuited polyphase winding, which acts as the secondary winding. There are two main types of rotor structures commonly used:

Squirrel-cage rotor: This rotor assembly resembles a cylindrical cage, with metal crowns connected at each end. Within the cage, there is a stack of sheets, and the motor's axis passes through the center.

Wound rotor: Similar to the squirrel-cage rotor, this rotor is also made up of stacked sheets. However, notches are made in the rotor to accommodate the winding. One end of the winding is connected to the end of the shaft through rings, while the other end is connected together at the midpoint of a star coupling. The brushes, also known as commutators, make contact with the rings, which are connected to the starting device (resistor).

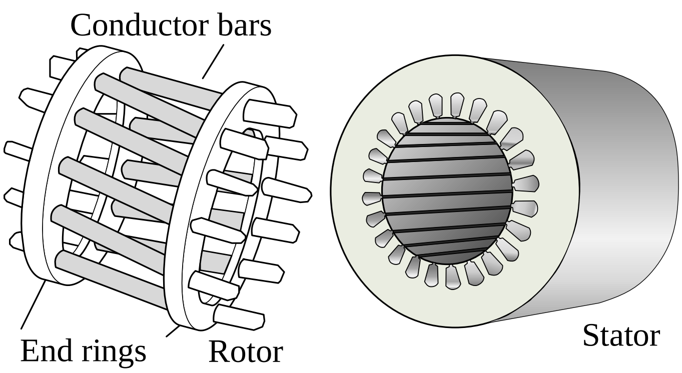

Figure 1.2 Stator and rotor configuration of an induction motor (IM).

Modeling the IM is crucial for simulating and understanding its behavior during transient states. By developing a model, we can gain insights into how the motor operates and devise effective control strategies. Throughout this chapter, we will delve into the various stages of the modeling process, explaining each step thoroughly.

1.2.2 Simplifying Assumptions

To make the modeling of an induction motor (IM) more manageable, we can make several simplifying assumptions. These assumptions are as follows:

- Constant air gap,
- Neglected notch effect,
- Sinusoidal spatial distribution of air gap magneto motive forces,
- Unsaturated magnetic circuit with constant permeability,
- Negligible ferromagnetic losses.

Overall, these simplifying assumptions allow us to create a simplified model of the induction motor that is easier to analyze and understand. While they may not capture all the intricacies and real-world behaviors of the motor, they provide a good starting point for studying its fundamental characteristics and performance.

1.3 The IM model

1.3.1Electrical equations

For the stator:

$$[V_S]_{ABC} = R_S[I_S]_{ABC} + \frac{d}{dt}[\Phi_S]_{ABC} \tag{1.1}$$

For the rotor:

$$[V_R]_{ABC} = R_R[I_R]_{ABC} + \frac{d}{dt}[\Phi_R]_{ABC} \tag{1.2}$$

1.3.2 Magnetic equations

The expressions for the totalized fluxes through the stator and rotor windings are written in matrix form as follows:

$$[\Phi_S]_{ABC} = [L_{SS}][I_S]_{ABC} + [L_{SR}]_{ABC}[I_R]_{ABC} \tag{1.3}$$

$$[\Phi_R]_{ABC} = [L_{RR}][I_R]_{ABC} + [L_{RS}]_{ABC}[I_S]_{ABC} \tag{1.4}$$

Such as:

$[V_S]_{ABC} = [V_{SA} \quad V_{SB} V_{SC}]^T$ Stator voltage vector.

$[I_S]_{ABC} = [I_{SA} I_{SB} I_{SC}]^T$ Stator current vector.

$[V_R]_{ABC} = [V_{RA} V_{RB} V_{RC}]^T$ Rotor voltage vector.

$[I_R]_{ABC} = [I_{RA} I_{RB} I_{RC}]^T$ Rotor current vector.

$$[\Phi_S]_{ABC} = [\Phi_{SA}\Phi_{SB}\Phi_{SC}]^T \qquad \text{Stator flux vector.}$$

$$[\Phi_R]_{ABC} = [\Phi_{RA}\Phi_{RB}\Phi_{RC}]^T \qquad \text{Rotor flux vector.}$$

with:

$$[L_{SR}] = [L_{RS}]^T$$

$$[L_{SS}] = \begin{pmatrix} l_S & m_S & m_S \\ m_S & l_S & m_S \\ m_S & m_S & l_S \end{pmatrix}, [L_{RR}] = \begin{pmatrix} l_R & m_R & m_R \\ m_R & l_R & m_R \\ m_R & m_R & l_R \end{pmatrix}$$

$$[L_{SR}] = m_{SR} \begin{pmatrix} \cos(\theta) & \cos(\theta + \frac{2\pi}{3}) & \cos(\theta - \frac{2\pi}{3}) \\ \cos(\theta - \frac{2\pi}{3}) & \cos(\theta) & \cos(\theta + \frac{2\pi}{3}) \\ \cos(\theta + \frac{2\pi}{3}) & \cos(\theta - \frac{2\pi}{3}) & \cos(\theta) \end{pmatrix}$$

L_{ss} : Stator inductance matrix.

L_{rr}: Matrix of rotor inductors.

L_{sr}: Matrix of the inductances mutual of the stator rotor coupling.

l_S, l_R: Self-inductance of the stator and rotor phases.

m_S: Mutual inductance between stator phases.

m_r: Mutual inductance between rotor phases.

1.3.3 Mechanical equations

The expression of the mechanical equation is given by:

$$T_e - T_l = J\frac{d}{dt}\Omega + f\Omega \tag{1.5}$$

J: moment of inertia of the rotor.

f: Viscous coefficient of friction.

T_e: Electromagnetic torque.

T_l: Load torque.

1.4 Park's transformation

Park's transformation facilitates the conversion of a three-phase system to a two-phase system. In this new reference frame, the parameters are represented differently [2]. This transformation is viewed as a replacement for the transition from a three-phase system to a two-phase system, as shown in Figure 1.3. As a result, we can obtain a system with constant coefficients.

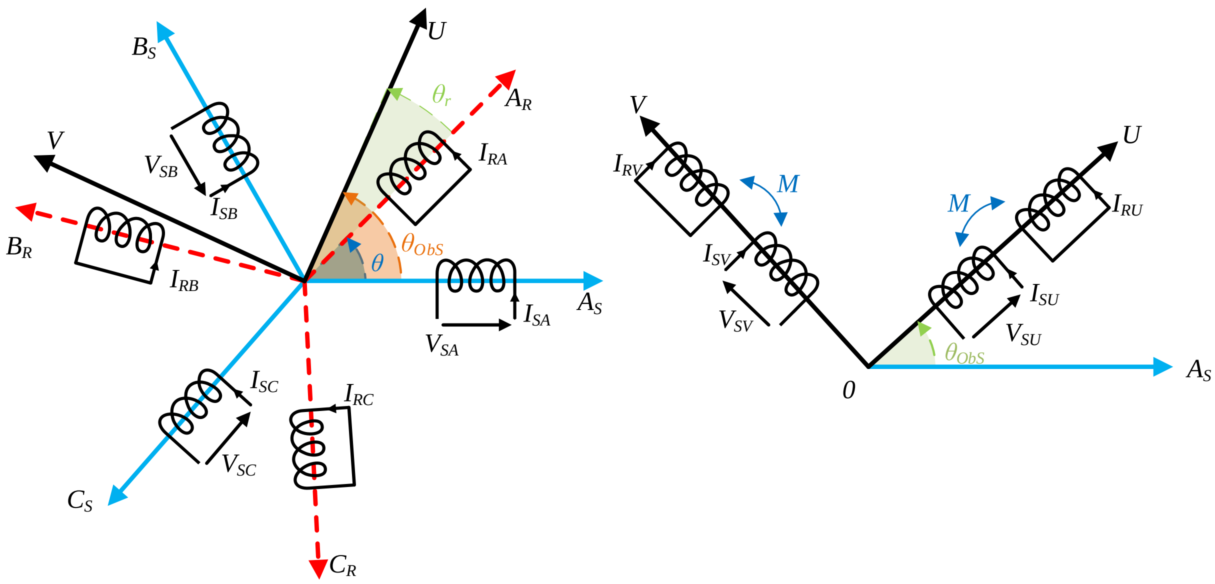

Figure 1.3 Representation of the three-phase model and its equivalent two-phase model for an induction motor (IM).

$$[P] = \sqrt{\frac{2}{3}} \begin{pmatrix} \cos(\theta) & \cos(\theta - \frac{2\pi}{3}) & \cos(\theta - \frac{4\pi}{3}) \\ \sin(\theta) & -\sin(\theta - \frac{2\pi}{3}) & -\sin(\theta - \frac{4\pi}{3}) \\ \frac{1}{\sqrt{2}} & \frac{1}{\sqrt{2}} & \frac{1}{\sqrt{2}} \end{pmatrix}$$

with:

θ: Angle between the magnetic axis and the longitudinal axis.

Applying Park's transformation to the electric and magnetic matrix models results in the following section.

1.4.1. Electrical equations

If we assume that all monopolar quantities are zero, we can transition from the three-phase system to the two-phase system (u, v) using the Park transformation.

$$V_{SU} = R_S I_{SU} + \frac{d\Phi_{SU}}{dt} - \omega_{ObS}\Phi_{SV}$$

$$V_{SV} = R_S I_{SV} + \frac{d\Phi_{SV}}{dt} + \omega_{ObS}\Phi_{SU}$$

$$0 = R_R I_{RU} + \frac{d\Phi_{RU}}{dt} - (\omega_{ObS} - \omega)\Phi_{RV} \tag{1.6}$$

$$0 = R_R I_{RV} + \frac{d\Phi_{RV}}{dt} + (\omega_{ObS} - \omega)\Phi_{RU}$$

1.4.2. Magnetic equations

$$\Phi_{SU} = L_S I_{SU} + M I_{RU}$$

$$\Phi_{SV} = L_S I_{SV} + M I_{RV}$$

$$\Phi_{RU} = L_R I_{RU} + M I_{SU} \tag{1.7}$$

$$\Phi_{RV} = L_R I_{RV} + M I_{SV}$$

with:

$L_S = l_S - m_S$: Inductance cyclique propre du stator.

$L_R = l_R - m_R$: Inductance cyclique propre du rotor.

$M = \frac{3}{2} m_{SR}$: Inductance cyclique mutuelle stator-rotor.

1.4.3. Mechanical equations

$$T_e - T_l = J\frac{d\Omega}{dt} + f\Omega$$

$$T_e = \frac{3}{2}\frac{Mp}{L_R}(\Phi_{RU} I_{SV} - \Phi_{RV} I_{SU}) \tag{1.8}$$

1.5. Choice of the reference two-phase frame

The model of the motor has been presented in a two-phase reference (U, V) with any orientation; however, there are different possibilities for choosing a system reference axis and it usually depends on the purposes of the application. The choice of the frame of reference practically brings us back to the three possible cases

- Axis marker (α, β): the two-phase system linked to the stator $\theta_{ObS} = 0$.
- Axis reference (d, q): the two-phase system linked to the rotating field $\theta_{ObS} = \theta_s$.
- Axis reference (x, y): the two-phase system linked to the rotor $\theta_{ObS} = \theta$.

with:

θ_s: Electrical angle of rotation of the rotating field.

1.5.1. Reference frame linked to the stator (*α, β*)

$$\omega_s = \frac{d\theta_s}{dt} = 0 \tag{1.9}$$

In addition, we replace the index "*u*" by "*α*" and "*v*" by "*β*", we obtain:

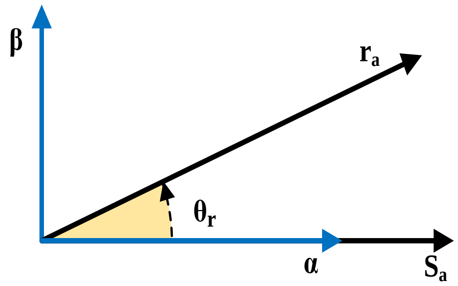

Figure1.4 Representation of the real axes of the induction motor (IM) with respect to the reference frame (α,β).

The equations of the IM in the frame (*α, β*) linked to the stator take the following form:

$$\begin{aligned} V_{S\alpha} &= R_S I_{S\alpha} + \frac{d\Phi_{S\alpha}}{dt} \\ V_{S\beta} &= R_S I_{S\beta} + \frac{d\Phi_{S\beta}}{dt} \\ 0 &= R_R I_{R\alpha} + \frac{d\Phi_{R\alpha}}{dt} + \omega_r \Phi_{R\beta} \\ 0 &= R_R I_{R\beta} + \frac{d\Phi_{R\beta}}{dt} - \omega_r \Phi_{R\alpha} \end{aligned} \tag{1.10}$$

This collection of data contains actual electric voltages and currents, which are suitable for analyzing the beginning and ending phases of AC machinery.

1.5.2 Referential linked to the rotating field (*d, q*)

$$\omega_c = \frac{d}{dt}\theta_s = \omega_s \tag{1.11}$$

We replace the index "*u*" by "*d*" and "*v*" by "*q*":

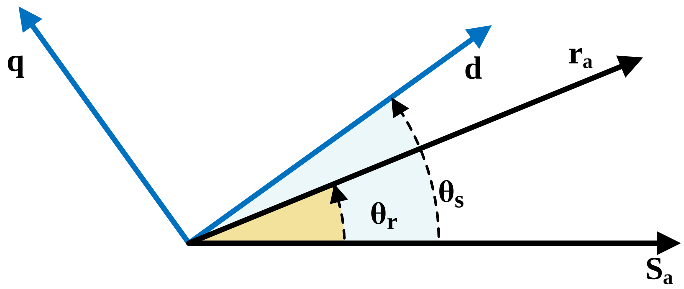

Figure 1.5 Representation of the model of induction motor in the reference frame (d.q).

The equations of the IM in the frame (d, q) related to the rotating field take the following form:

$$\begin{aligned} V_{Sd} &= R_S I_{Sd} + \frac{d\Phi_{Sd}}{dt} - \omega_S \Phi_{Sq} \\ V_{Sq} &= R_S I_{Sq} + \frac{d\Phi_{Sq}}{dt} + \omega_S \Phi_{Sd} \\ 0 &= R_R I_{Rd} + \frac{d\Phi_{Rd}}{dt} - (\omega_S - \omega)\Phi_{Rq} \\ 0 &= R_R I_{Rq} + \frac{d\Phi_{Rq}}{dt} + (\omega_S - \omega)\Phi_{Rd} \end{aligned} \tag{1.12}$$

$$\begin{aligned} \Phi_{Sd} &= L_S I_{Sd} + M I_{Rd} \\ \Phi_{Sq} &= L_S I_{Sq} + M I_{Rq} \\ \Phi_{Rd} &= L_R I_{Rd} + M I_{Sd} \\ \Phi_{Rq} &= l_R I_{Rq} + M I_{Sq} \end{aligned} \tag{1.13}$$

By transferring from equation (1.13) the quantities: $\Phi_{Sd}\Phi_{Sq}\Phi_{Rd}\Phi_{Rq}$ In the system (1.12), the model of the IM becomes:

$$\begin{aligned} V_{Sd} &= \sigma L_S I_{Sd} - \omega_S \sigma L_S I_{Sq} + \frac{M}{L_R T_R}\Phi_{Rq} \\ V_{Sq} &= \sigma L_S I_{Sq} + \omega_S \sigma L_S I_{Sd} + \frac{M}{L_R}\omega_S \Phi_{Rd} \\ 0 &= \frac{1}{T_R}\Phi_{Rd} - \frac{M}{T_R} i_{Sd} + \frac{d\Phi_{Rd}}{dt} - \omega_R \Phi_{Rq} \\ 0 &= \frac{1}{T_R}\Phi_{Rq} - \frac{M}{T_R} i_{Sq} + \frac{d\Phi_{Rq}}{dt} + \omega_R \Phi_{Rd} \end{aligned} \tag{1.14}$$

Using this frame of reference offers the benefit of having continuous variables in a state of equilibrium, which can facilitate the process of regulating them Φ_{Sd}.

1.5.3 Reference frame linked to the rotor (x, y)

It results in the condition:

$$\omega_c = \frac{d}{dt}\theta_r = \omega_r \tag{1.15}$$

we replace the index "u" by "x" and "v" by "y"

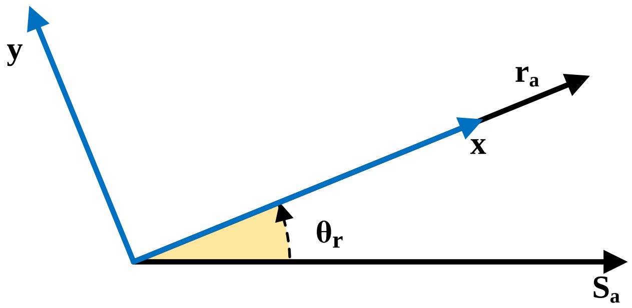

Figure 1.6 Comparison of the real axes of the induction motor (IM) with the reference frame (x y).

The equations describing the IM in the rotor-related (x, y) frame can be expressed in the following manner:

$$\begin{aligned} V_{SX} &= R_S I_{SX} + \frac{d}{dt}\Phi_{SX} - \omega_r \Phi_{SY} \\ V_{SY} &= R_S I_{SY} + \frac{d}{dt}\Phi_{SY} + \omega_r \Phi_{SX} \\ V_{RX} &= 0 = R_R I_{RX} + \frac{d}{dt}\Phi_{RX} \\ V_{RY} &= 0 = R_R I_{RY} + \frac{d}{dt}\Phi_{RY} \end{aligned} \tag{1.16}$$

This setup is utilized for examining temporary processes in both synchronous and asynchronous machines.

1.7 State Equation of IM

There exist multiple methods for placing the motor model in a particular state, with the specific form being contingent upon factors such as the type of power source, the command quantities, the chosen reference frame, and the system outputs along with its state variables.

In this investigation, we examine a voltage-controlled machine, wherein the motor's model must take in the stator voltage components on the α and β axes as inputs. The state variables to be considered shall be the stator currents and the rotor flux, since the stator currents are easily measurable and enable the observation of the rotor flux. The mechanical speed and rotor flux are the quantities that require regulation. Considering this selection, the system (I-14) can be expressed in the following arrangement:

$$\begin{aligned} \frac{dI_{S\alpha}}{dt} &= \left(\frac{1}{T_s\sigma} + \frac{1}{T_R\sigma}\right) I_{s\alpha} + \frac{1}{MT_R\sigma}\Phi_{R\alpha} + \frac{1-\sigma}{M\sigma}\omega\Phi_{R\beta} + \frac{1}{\sigma L_S}V_{S\alpha} \\ \frac{dI_{S\beta}}{dt} &= -\left(\frac{1}{T_s\sigma} + \frac{1}{T_R\sigma}\right) I_{s\beta} - \frac{1-\sigma}{M\sigma}\omega\Phi_{R\alpha} + \frac{1-\sigma}{MT_R\sigma}\Phi_{R\beta} + \frac{1}{\sigma L_S}V_{S\beta} \end{aligned} \tag{1.17}$$

$$\frac{d\Phi_{R\alpha}}{dt} = \frac{M}{T_R} I_{S\alpha} - \frac{1}{T_R}\Phi_{R\alpha} - \omega\Phi_{R\beta}$$

$$\frac{d\Phi_{R\beta}}{dt} = \frac{M}{T_R} I_{S\beta} - \frac{1}{T_R}\Phi_{R\beta} + \omega\Phi_{R\alpha}$$

with:

$$T_R = \frac{L_R}{R_R}\text{: Rotor time constant.}$$

$$T_S = \frac{L_S}{R_S}\text{: Stator time constant.}$$

$$\sigma = 1 - \frac{M^2}{L_S L_R}\text{: Leakage coefficient.}$$

$$\dot{X} = AX + BU \tag{1.18}$$

with:

$[X] = [I_{S\alpha} \quad I_{S\beta} \quad \Phi_{R\alpha} \quad \Phi_{R\beta}]^T$: State Vector.

$[U] = [V_{S\alpha} \quad V_{S\beta}]^T$: Control Vector .

$[A]$: System state evolution matrix.

$[B]$: Control System Matrix.

$$[A] = \begin{bmatrix} -\left(\frac{1}{\sigma T_S} + \frac{1-\sigma}{\sigma T_R}\right) & 0 & \frac{1-\sigma}{M\sigma T_R} & \frac{1-\sigma}{M\sigma}\omega \\ 0 & -\left(\frac{1}{\sigma T_S} + \frac{1-\sigma}{\sigma T_R}\right) & -\frac{1-\sigma}{M\sigma}\omega & \frac{1-\sigma}{M\sigma T_R} \\ \frac{M}{T_R} & 0 & -\frac{1}{T_R} & -\omega \\ 0 & \frac{M}{T_R} & \omega & -\frac{1}{T_R} \end{bmatrix}$$

$$[B] = \begin{bmatrix} \frac{1}{\sigma L_S} & 0 \\ 0 & \frac{1}{\sigma L_S} \\ 0 & 0 \\ 0 & 0 \end{bmatrix}$$

While this model accurately depicts the motor's functioning, it accentuates the non-linearities and the substantial interdependence between the state variables, leading to a complex control scheme necessary for achieving optimal performance from the machine.

1.8. Pulse Width Modulation Technique (PWM)

The PWM strategy is widely utilized to control induction motors and is commonly employed in static converters. Multiple approaches have been devised to generate a sinusoidal voltage at the output of the inverter, while keeping the harmonic content to a minimum. This strategy operates by dividing the sampling period into intervals or modulation durations, and assigning specific time durations to each voltage vector. Through precise control of the converter components' on and off times, the PWM strategy effectively reduces the harmonics present in the applied voltages of the motor. This technique ensures smoother operation and improved performance of the induction motor [5].

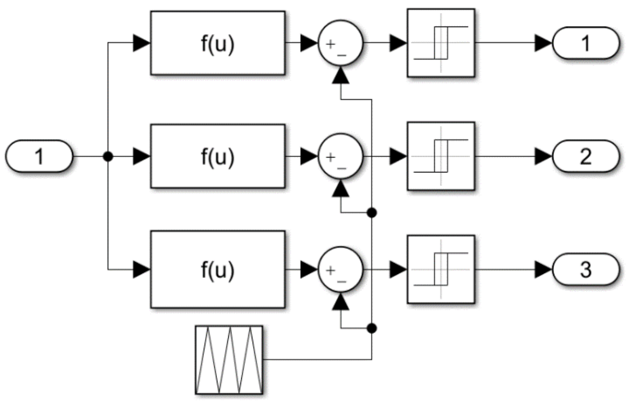

Figure 1.7 Simulation block diagram of the PWM (Pulse Width Modulation) technique.

1.9 Simulation results and interpretation

In the context of Simulink, a block for the induction motor in MATLAB refers to a computational component or module that represents the behavior and characteristics of an induction motor within a Simulink model. Simulink is a graphical programming environment within MATLAB that allows for the simulation and modeling of dynamic systems, including electrical machines like the induction motor.

The Simulink block for the induction motor typically encapsulates the mathematical equations and algorithms that govern the motor's operation, such as the electrical, mechanical, and control dynamics. It takes input signals, such as voltage and current, and produces output signals, such as speed and torque, based on the defined motor model and associated parameters.

The block includes various configurable parameters, such as the motor's electrical and mechanical parameters, control strategies, and simulation settings. Users can modify these parameters to customize the behavior of the induction motor within their Simulink model, allowing for the analysis and optimization of motor performance in different scenarios.

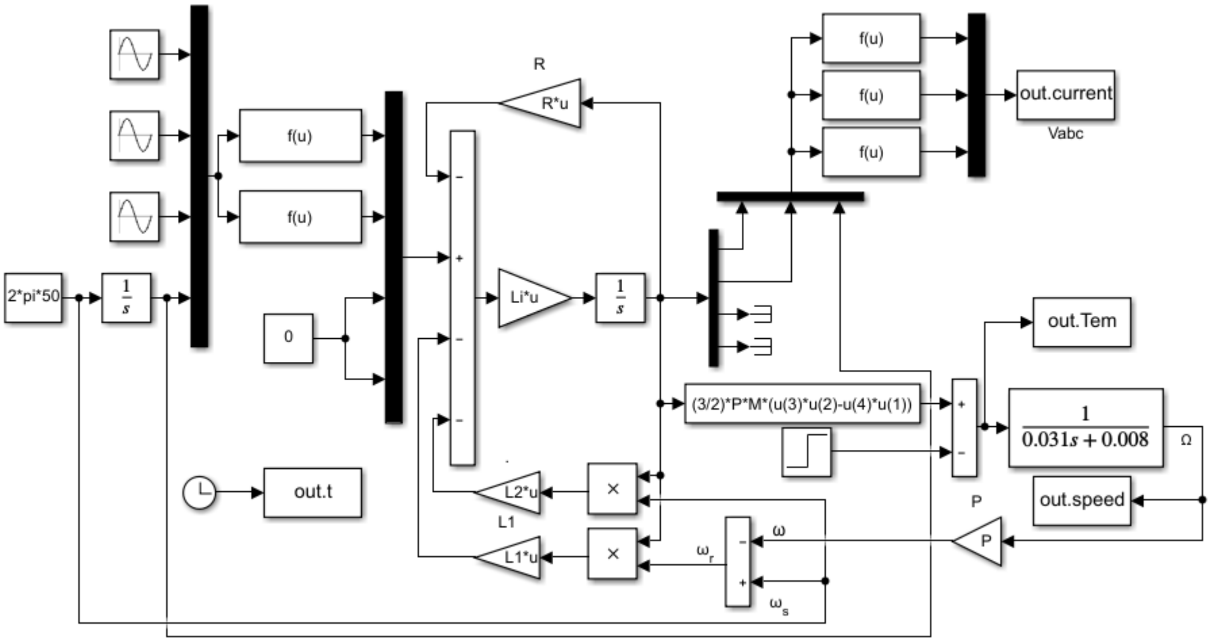

Figure 1.8 Simulation block of the IM supplied with load voltage.

1.9.1 Simulation results

The simulation results provided by Figures (1.9, 1.10, 1.11) depict the changes in key parameters of the induction motor, namely the rotor speed, electromagnetic torque, stator currents, and rotor flux. The simulation was conducted for a no-load start followed by a load (T_l =10N.n) variation at time t = 0.8s.

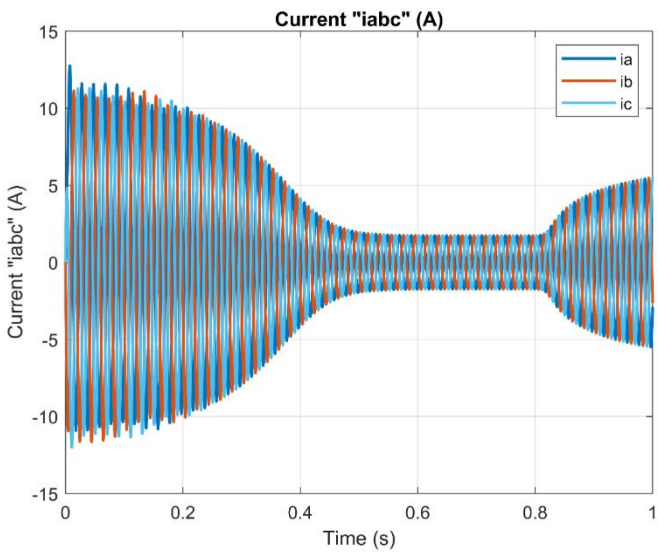

Figure1.9 Stator currents in the abc frame of the induction motor (IM).

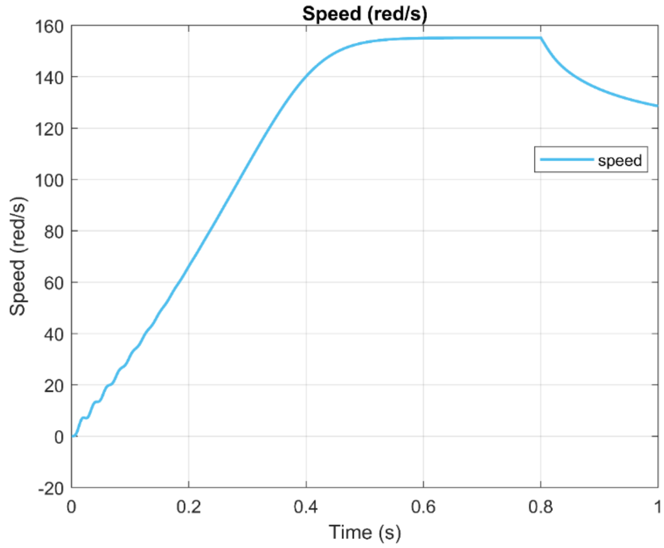

Figure.1.10 Rotor speed of the induction motor (IM).

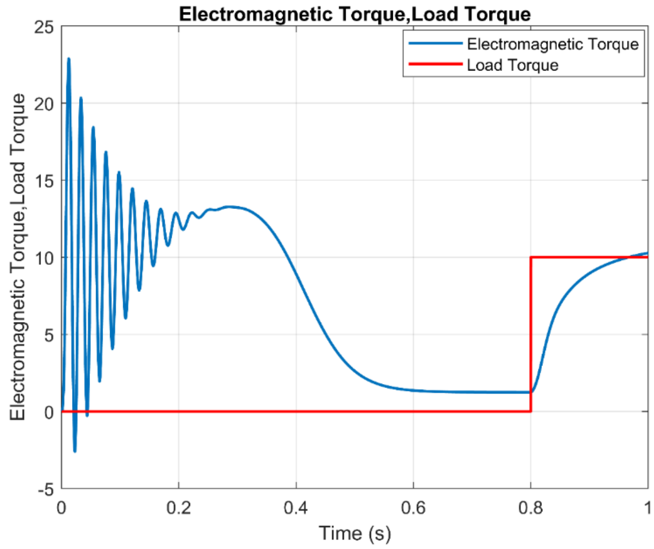

Figure.1 .11 Electromagnetic torque of the induction motor (IM).

The simulation results show a clear pattern in the speed behavior. Initially, the speed increases linearly and then approaches the synchronous speed of 157 rad/s. Additionally, the investigation indicates that the electromagnetic torque reaches its highest value during the early phase, leading to a significant current consumption. However, it gradually decreases to a steady level when there is no load. Importantly, when a load of 10N.m is applied, the speed noticeably decreases, and a stable level of electromagnetic torque is established, corresponding to the magnitude of the applied load.

1.11 Conclusion

The present section discusses a crucial aspect of analyzing induction motors, specifically focusing on the Park model for motor modeling. This model provides a simplified portrayal of the motor, reducing the intricacies associated with the three-phase model. However, it is important to recognize that despite these simplifications, there is a significant interdependence between the stator and rotor variables, which can create difficulties in motor control.

To address these challenges and enhance the motor's dynamic performance, the following section will introduce scalar control and vector control techniques. These methods aim to improve control effectiveness and optimize the overall motor performance.

Chapter 2

Scalar and Field-Oriented Control of Induction Motor

Introduction

The control of induction motors, specifically through scalar and field-oriented approaches, is a crucial topic in the realm of industrial applications that require high torque performance and variable speed. The combination of induction motors and static converters has become the preferred choice for such applications. The growing popularity of this combination can be largely attributed to significant advancements in power electronic components. These advancements have facilitated the development of static converters that possess fast-switching capabilities and high power output. As a result, these converters offer improved flexibility in power supply by allowing adjustable wave amplitude and frequency [9].

Furthermore, the introduction of highly efficient digital signal processors (DSPs) has played a major role in the widespread adoption of this technology. DSPs have made it possible to implement sophisticated control laws at reduced costs. By utilizing the computational capabilities of DSPs, complex control algorithms can be executed efficiently, enabling precise control of induction motors and optimization of their performance [9].

This chapter aims to provide a comprehensive understanding of the fundamental principles and techniques behind scalar and field-oriented control of induction motors. It will delve into the underlying concepts required to achieve accurate torque control and variable speed operation. By gaining knowledge of these control strategies, engineers and researchers can fully utilize the potential of induction motors combined with static converters, effectively meeting the demanding requirements of industrial applications.

I.1 Scalar control (*V/f* control)

Scalar control is a straightforward and traditional control technique for an IM that is suitable for applications that only need average static or dynamic performance. This control mode is still popular due to recent advancements in power electronics, and it is commonly used in various industrial applications, such as pumping, air conditioning, and ventilation.

The scalar control method for an IM is a simple and old control technique that imposes the voltage or current modulus and pulsation on the motor's armature terminals. This technique is commonly used in applications that require average static or dynamic performance and is now prevalent due to advances in power electronics. The scalar control technique has several variations, which depend on whether it is applied to the current or voltage and the actuator topology (voltage or current inverter). In voltage supply, the inverters provide independent voltages with respect to the load, while in the current supply; the supplied currents are influenced by the load's nature, resulting in various shapes and amplitudes.

The method of controlling the speed involves adjusting the stator pulse emitted by the regulator. This technique is based on the steady-state model of the motor [6].

2.3. Operating principle of scalar control

This is one of the initial control techniques that was designed for changing the speed of IM. The focus of this method is only on the magnitude of the controlled variable and not its phase [7].

There are different scalar control methods that can be used based on whether the current or voltage inverter is used, and they mainly depend on the actuator topology. Among the various options, the voltage inverter is the most common for small and medium power applications. The "*V/f* " control technique is frequently used, and it maintains a constant ratio between the voltage and frequency. This implies that the flux is also constant, which is represented by the equation " $r = Vs / \omega_s$ = Cts" The slip can be controlled to achieve torque control.

Assuming low slip and ignoring stator resistance voltage drop, the torque in a static state can be calculated using the following equation:

$$T_e = 3 \frac{p}{R'_r} \left(\frac{V_s}{\omega_s} \right)^2 \omega_{sl} \tag{2.1}$$

with:

ω_{sl}: slip pulse.

ω_s : stator pulse.

V_s : stator voltage.

R'_r : Rotor resistance reduced to stator

p : pair of the pole.

In the chapter on scalar control of induction motors, we begin by exploring an important equation that establishes a relationship between torque and the square of the voltage-to-stator frequency ratio. This equation highlights the direct proportionality between torque and the square of this ratio. When the flux is maintained at a constant level, the control characteristic resembles that of a steady-state DC machine, with the slip frequency taking on the role of the armature current [8].

To gain a better understanding of this concept, let's consider a simple function where the ratio of voltage to stator frequency (V/f) is kept constant. In such a scenario, it becomes evident that the maximum torque remains constant. This behavior can be visualized in the accompanying figure, which provides a clear illustration of the relationship between torque and the constant V/f ratio [8].

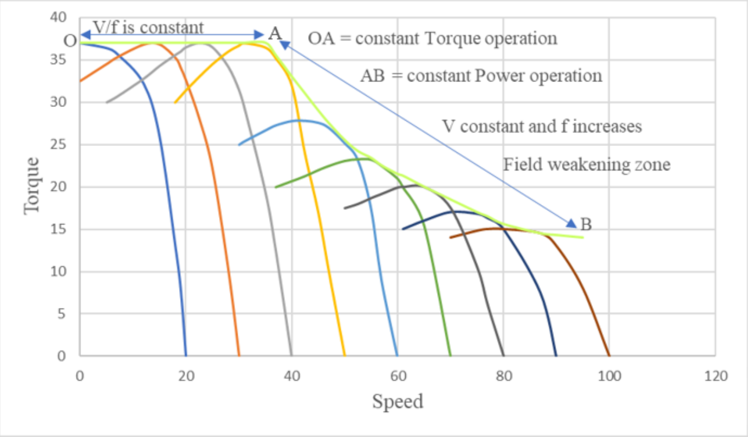

Figure 2.1 Speed-Torque characteristics of V/f Control.

By examining the torque characteristics and the influence of voltage and frequency ratios, we can gain valuable insights into controlling and optimizing the performance of induction motors in various applications. Therefore, maintaining a constant "*V/f* " ratio ensures a constant flux in the machine.

$$\frac{V}{f} = cst \Rightarrow \begin{cases} \Phi = cst \\ Te_{max} = cst \end{cases} \Omega \leq \Omega_n \tag{2.2}$$

When the machine is operated at speeds higher than its rated speed, the voltage is kept at its highest level, but the frequency is increased by reducing the "V/f" ratio. This adjustment leads to a reduction in the machine's torque output.

Conversely, at low speeds, it is important to consider the voltage drop across the stator resistance, as it becomes significant. To counteract this voltage drop, a compensation term V0 is introduced. This compensation term helps to compensate for the voltage decrease and ensure that the motor operates effectively at low speeds.

Scalar control is a technique used to control the speed of induction motors by manipulating the voltage and frequency supplied to the motor. By adjusting the voltage and frequency in a coordinated manner, the motor's speed can be regulated across a wide range of operating conditions.

In scalar control, when the motor operates above its rated speed, the voltage is maintained at its maximum value to provide sufficient power to drive the motor. However, the frequency is increased while keeping the voltage constant, which reduces the V/f ratio. This reduction in the V/f ratio results in a decrease in the torque produced by the motor.

At lower speeds, the voltage drop across the stator resistance becomes significant. To compensate for this voltage drop and ensure proper motor operation, a compensation term V0 is added. This compensation term effectively increases the voltage supplied to the motor, compensating for the voltage drop and enabling the motor to operate efficiently at low speeds.

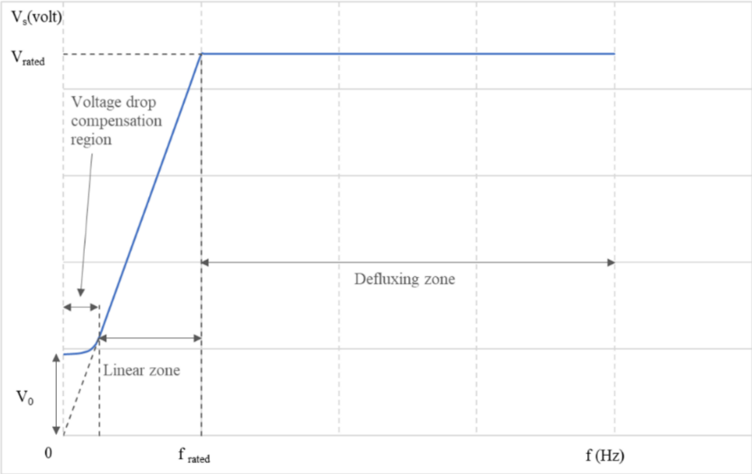

Figure 2.2 Scalar Law for the induction motor.

2.4. Advantages and disadvantages of scalar control

The advantages and disadvantages of scalar control for induction motors are:

2.4.1 The advantages

- The method allows for a large range of speed variation.
- The method provides increased stability.
- The ease of implementing the steady state control laws.

2.4.2 Disadvantages

- The control law has limitations, including instability in transient states of high amplitudes, such as starting and reversing the direction of rotation.
- The control law also faces problems at low speeds due to the drop in "$Rs\ Is$".
- It is based on the steady state model and has slow dynamics.
- The control law can only control magnitudes in amplitude, and not in phase.

2.5 Regulator calculation

The speed control loop with a PI (Proportional-Integral) structure is a commonly employed method for regulating the speed of a system. The placement pole technique is often utilized in the design process of such control loops. It involves strategically determining the location of the poles within the control system to achieve the desired performance and stability. By using this method, engineers can systematically tune the parameters of the controller and optimize the overall speed control loop.

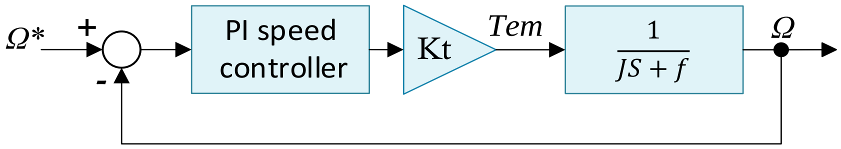

Figure 2.3 Speed control loop with a PI (Proportional-Integral) structure.

The PI and the speed transfer function are respectively given as

$$C_{\Omega}(S) = K_{p\Omega}\frac{T_{i\Omega}S+1}{T_{i\Omega}S} \tag{2.3}$$

$$\Omega TF = \frac{(Kt/f)}{(J/f)S+1} \tag{2.4}$$

with

$$T_{i\Omega}\,S+1 = (J/f)S+1 \tag{2.5}$$

The open-loop transfer function $C_{\Omega OL}(S)$ is given by

$$C_{\Omega OL}(S) = \frac{K_{p\Omega}Kt}{fT_{i\Omega}S} \tag{2.6}$$

The closed loop transfer function $C_{\Omega CL}(S)$ is a first order of the following form:

$$C_{\Omega CL}(S) = \frac{1}{\frac{fT_{i\Omega}}{K_{p\Omega}Kt}S+1} \tag{2.7}$$

with a time constant fixing the behavior in closed loop is

$$T_{0\Omega} = \frac{fT_{i\Omega}}{K_{p\Omega}Kt} \leq \frac{J}{n_{\Omega}f} = \frac{1}{\omega_{cc_{\Omega}}} \tag{2.8}$$

$$K_{p\Omega} = \frac{fn_{\Omega}}{Kt} \tag{2.9}$$

$$T_{i\Omega} = \frac{K_{p\Omega}}{K_{i\Omega}} = T_{0\Omega}n_{\Omega} \tag{2.10}$$

$$K_{i\Omega} = \frac{K_{p\Omega}}{T_{0\Omega}n_{\Omega}} = \frac{f^2n_{\Omega}}{JKt} \tag{2.11}$$

$$Kt = \frac{3PV^2}{R'_r f^2} \tag{2.12}$$

$$R'_r = \frac{Ls^2Rr}{M^2} \tag{2.13}$$

n_{Ω}: speed gain improvement coefficient

$\omega_{cc_{\Omega}}$: speed gain cross_over frequency

2.6 Simulation of the scalar control of the IM

In this section, we conducted a simulation of an inducion motor operating with a PWM voltage inverter and being controlled by scalar control. The simulation was performed in two different operating modes: without a load and with a load.

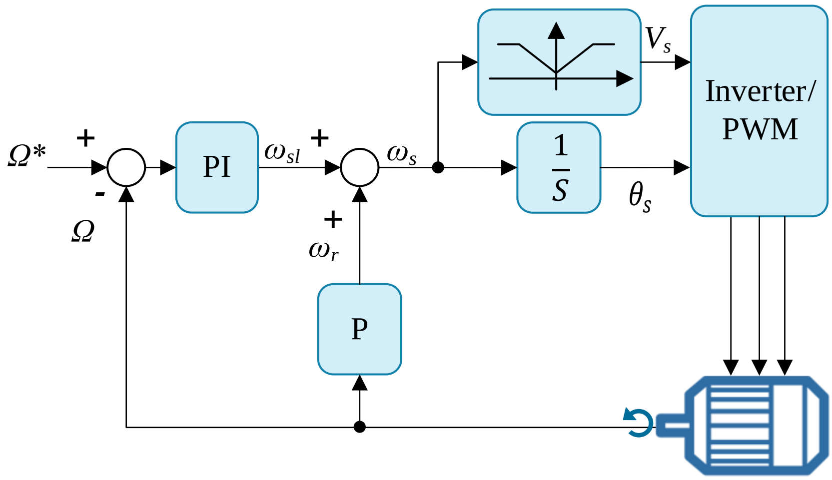

Figure 2.4 Diagram of the scalar control implementation for the induction motor (IM).

2.6.1. Simulation results

In this section, we will simulate the scalar control of an induction motor (IM) that is powered by a two-level inverter. It is important to mention that the simulation is performed under specific conditions, which involve a variable reference speed ranging from 0 to 100 rad/s. Additionally, a load torque of 10 Nm is applied at different time intervals throughout the simulation.

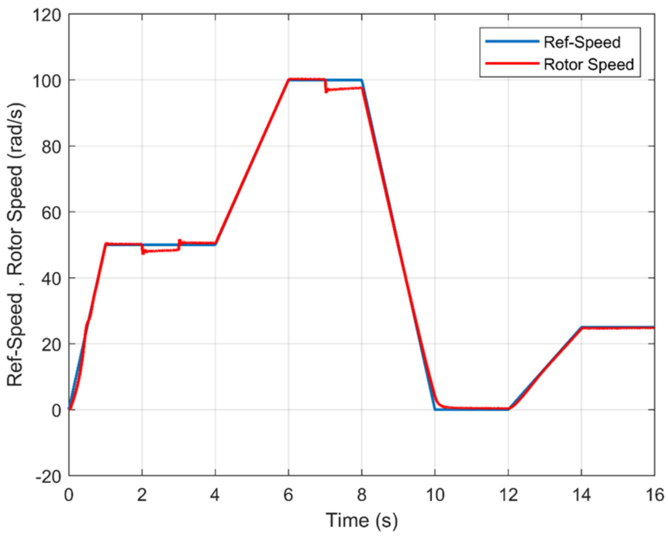

Figure 2.5 Diagram of speed simulation over time.

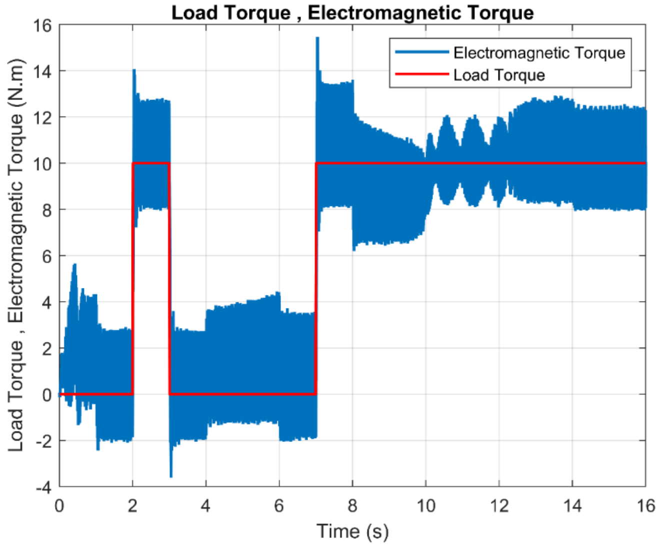

Figure 2.6 Diagram of electromagnetic torque simulation over time

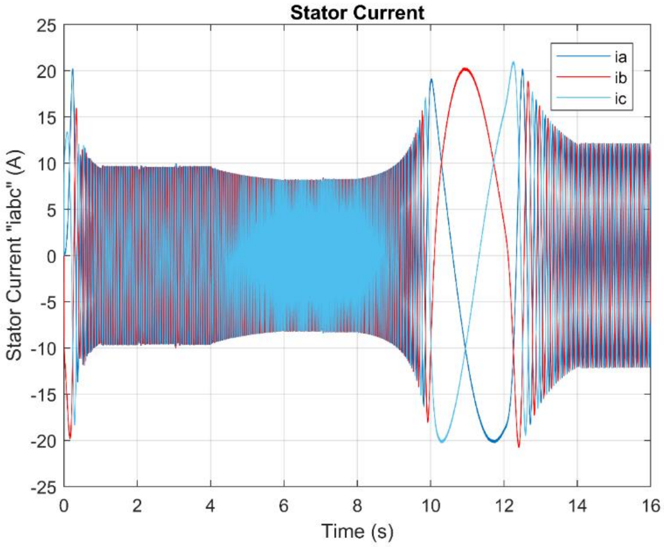

Figure 2.7 Diagram of stator current simulation over time.

The machine initiates its operation without any load, starting from t=0 with a speed of 0 rad/s and gradually increasing to a speed of 50 rad/s by t=1s. It follows the reference speed in a smooth oscillating manner. Consequently, the machine generates a torque of 2 N.m, aided by a momentary current during startup to achieve the required torque. Subsequently, it stabilizes at a current of 9 A. However, due to the imprecise nature of scalar control at low and zero speeds, there is some fluctuation in the system. Once the speed stabilizes at 50 rad/s, the torque is balanced.

When a load torque of 10 N.m is applied at t=2s, it is observed that the torque increases by the same value (10 N.m). The current remains constant, and the speed experiences a slight decrease before returning to the reference value. Between t=8 and t=10, the speed gradually decreases from 100 rad/s to 0 rad/s, matching the reference. During this period, the torque fluctuates and decreases until it reaches 7 N.m, which signifies the braking process.

In general, scalar control tends to be less accurate at low speeds and zero speeds.

II. Field -Oriented control (FOC)

Vector control is a method of controlling an induction motor (IM) that has been around for a while. However, it was not until advancements in microelectronics that it could be effectively implemented and used. This is because vector control requires calculations such as Park transforms, trigonometric evaluations, and integrations, which were difficult to perform in pure analog.

The goal of vector control is to control the IM in a similar way as a DC motor with separate excitation. This is possible because the flux control (excitation current) and the torque control (armature current) are naturally decoupled in a DC motor (DCM), leading to a very quick torque response [3].

This chapter aims to provide an overview of the vector control method that is based on rotor flux orientation. It will begin by explaining the principles of this method, followed by the application of vector control to an IM model, where the machine's current, flux, and speed will be adjusted using PI-type regulators. Lastly, simulation results will be presented, along with robustness tests.

2.9 Principle of oriented flux vector control

To control the IM, it is essential to control the torque, speed, and position. However, the most fundamental control is that of the currents, which directly affects the torque. It is because the torque can be expressed as a cross product of the currents or fluxes in the (*d*-*q*) frame.

$$T_{em} = \frac{PM}{L_r}(\varphi_{rd} i_{sq} - \varphi_{rq} i_{sd}) \tag{2.14}$$

The formula for the electromagnetic torque in an IM is complex and does not have the natural decoupling that is present in a direct current machine. This makes controlling the torque and flux more difficult. However, vector control can solve this problem by decoupling the flux and torque. By eliminating the second product (φ_{rq}, I_{sq}), we can make the coupler similar to that of a direct current machine. This can be achieved by orienting the reference frame (*d*-*q*) in such a way that the quadrature flux component is cancelled out. This means that the rotor flux is entirely carried on the direct axis (*d*), and φ_{rq} = 0 and φ_{rd} = 1. The resulting torque equation becomes similar to that of a direct current machine [3].

$$T_{em} = \frac{PM}{L_r}(\varphi_r i_{sq}) \tag{2.15}$$

To adjust the flux, one can act on the i_{sd} component of the stator current, and to adjust the torque, one can act on the i_{sq}component. This creates two action variables similar to a DCM. One approach is to maintain the i_{sq} component constant by setting the reference to impose a nominal flux in the motor. The current regulator for i_{sd} is responsible for maintaining the current constant and equal to the reference i_{sd}^*.

According to [8], the orientation of the axes can be determined based on the flux directions in the motor, including the rotor flux, stator flux, or magnetizing flux (air gap).

Rotor flux: $\varphi_{rd} = \varphi_r$ et $\varphi_{rq} = 0$

Stator flux: $\varphi_{sd} = \varphi_s$ et $\varphi_{sq} = 0$

Air gap flux : $\varphi_{\eta d} = \varphi_\eta$ et $\varphi_{\eta q} = 0$

Assuming the axis is always aligned with the rotor flux vector, as illustrated in Eq.(2.16), the following holds true:

$$\begin{gathered} \varphi_{rd} = \varphi_r \\ \varphi_{rq} = 0 \end{gathered} \tag{2.16}$$

The result is expressed as the following torque equation:

$$T_{em} = \frac{PM}{L_r}(\varphi_r i_{sq}) \tag{2.17}$$

The orientation of the rotor flux is depicted in the following figure:

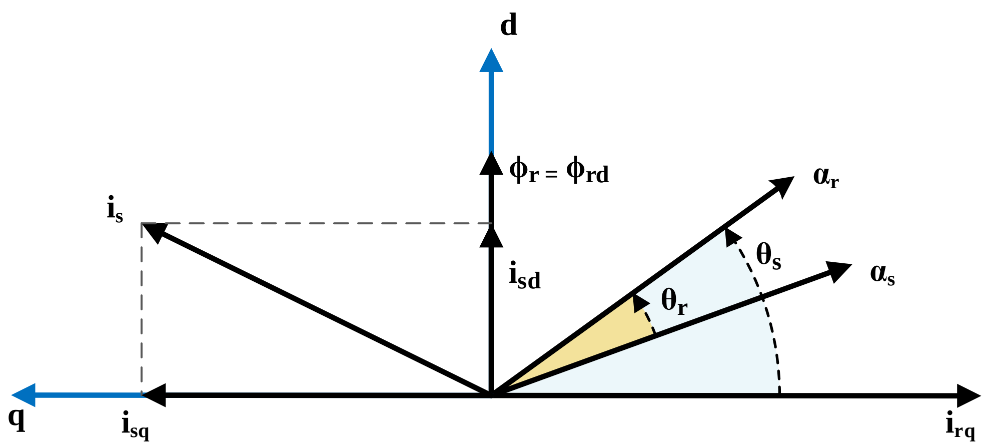

Figure 2.8 Rotor flux orientation.

By inserting the constant $K = P\frac{M^2}{L_r}$ into equation (2.18), we obtain:

$$T_{em} = K i_{sd} i_{sq} \tag{2.18}$$

Equation (2.18) is similar to the torque equation of a direct current DC motor. Therefore, the brush-collector system in a DC motor is substituted by the autopilot system in an IM to achieve synchronization between the rotor-induced current frequency and the rotational frequency, satisfying the following equation:

$$\omega_s = \omega + \omega_r = P\Omega + \omega_r$$

$$\theta_s = \int \omega_s dt$$

Two methods can be employed to achieve vector control of an IM: Direct FOC control, which was created by F. Blaschke, and Indirect FOC control, which was developed by K. Hass [8] [3].

2.10 Direct FOC control

Direct field-oriented control (FOC) requires knowledge of the magnitude and phase of the rotor flux at all times. One method to obtain this information is to measure the flux directly using sensors placed in the air gap. However, this method is challenging due to the harsh operating environment and the need for variable frequency filtering to remove noise caused by notches. Additionally, the installation of flux sensors increases the manufacturing cost of the motor.

An alternative approach is to estimate or observe the flux from conventional measurements such as currents, voltages, and speed. The use of such measurements can lead to a fully decoupled vector control design, which offers several advantages over traditional FOC methods. For example, fully decoupled vector control is more robust to noise and disturbances and can achieve higher performance in speed and torque control [1].

Here are some additional details about the two methods of obtaining the rotor flux:

Direct measurement: This method involves placing sensors in the air gap between the stator and rotor of the motor. The sensors measure the magnetic field strength, which can then be used to calculate the magnitude and phase of the rotor flux. This method is accurate and reliable, but it is also expensive and can be difficult to implement in some cases.

Estimation: This method uses conventional measurements such as currents, voltages, and speed to estimate the magnitude and phase of the rotor flux. This method is less accurate than direct measurement, but it is also less expensive and easier to implement.

The choice of which method to use depends on the specific application. For high-performance applications where accuracy is critical, direct measurement is the preferred method. For lower-performance applications where cost and complexity are more important, estimation can be a viable option.

2.11 Indirect FOC control

Indirect vector control is a type of control that does not involve flux adjustment. It does not require flux sensors, estimators, or observers. However, it requires the measurement of the rotor position since there is no knowledge of the modulus and phase of the rotor flux. Although this type of control is simpler, it has lower performance than direct control due to its sensitivity to variations in the rotor time constant. The advantage of this control is that it requires less computation in the microprocessor.

2.12 Principle of direct vector control with oriented rotor flux

The implementation of the rotor flux vector control we use involves orienting the rotating frame of axes (d, q) such that the d-axis aligns with the direction of the rotor flux vector φ_r. The flux φ_r is then oriented along the d-axis.

$$\begin{cases} v_{sd} = \sigma Ls\dfrac{di_{sd}}{dt} + R_t i_{sd} - \sigma L_s \omega_s i_{sq} - \dfrac{M}{L_r T_r}\varphi_r \\ v_{sq} = \sigma Ls\dfrac{di_{sq}}{dt} + R_t i_{sq} + \sigma L_s \omega_s i_{sd} + \dfrac{M}{L_r}\varphi_r \\ \varphi_r + T_r\dfrac{d\phi_r}{dt} = M i_{sd} \\ \omega_r = \dfrac{M i_{sq}}{\varphi_r T_r} \\ T_{em} = P\dfrac{M}{L_r}\varphi_r i_{sq} \end{cases} \tag{2.19}$$

The main goal of decoupling by compensation is to minimize the impact of input on multiple outputs. This involves modeling the system as a collection of single-variable systems that evolve independently, making the commands non-interactive. Various techniques can be employed for this purpose, including:

2.13 Principle of decoupling by compensation

The goal is to minimize the impact of input on multiple outputs and represent the system as a collection of single-variable systems that evolve independently, resulting in non-interacting controls. There are various methods available to achieve this objective.

- Decoupling using a regulator.
- A decoupling by state feedback.
- A decoupling by compensation, in which we are interested.

2.14 The current feedback loop

The current servo loop for I_{sd} and I_{sq} is established using a PI controller, which is responsible for achieving satisfactory dynamics.

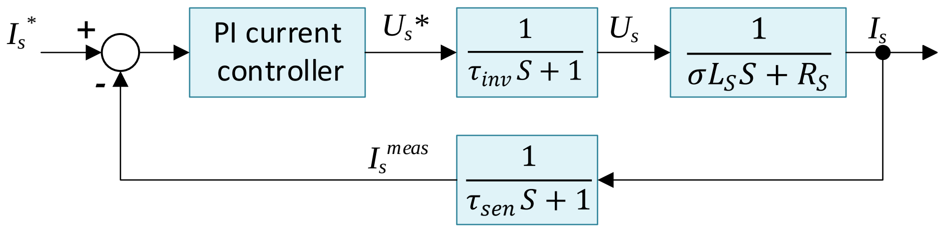

Figure 2.9 Simplified stator current control loop (Isd and Isq).

2.15 The speed feedback loop

In this depiction, we have presented vector control as speed control on the load side. The control diagram is shown as follows:

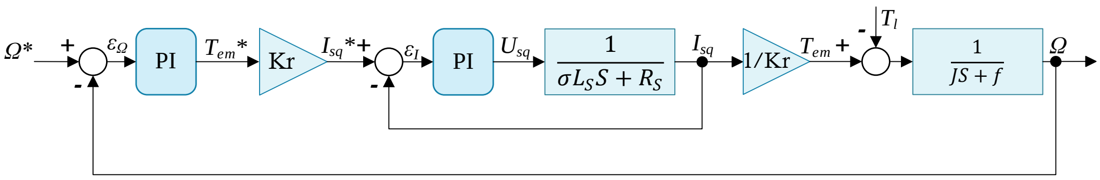

Figure 2.10 Speed control loop.

The controlled system includes an internal current loop, Isq, which is treated as a measurable disturbance in this context. The PI controller in the external speed loop is responsible for establishing the desired dynamics for the rotation speed, with the control variable Isq serving as the set point for the internal current loop. All of these controllers are depicted in the block diagram shown in Figure 2.10.

A portion of the inherent noise resulting from the presence of the inverter is represented by a first-order transfer function with a time constant of τ_{inv}, while the current sensor is represented by a first-order transfer function with a time constant of τ_{sen}. It is assumed that these two-time constants are significantly smaller compared to the time constant of the system, denoted as

$$\tau_{sys} = \left(\left(L_s - \frac{L_m^2}{L_r}\right)/R_s\right)$$

One note :

$$\frac{U_s^{ref}}{U_s} \approx 1 \text{ et } \frac{I_s^{meas}}{I_s} \approx 1$$

As a result, the diagram illustrating the stator current control loop is transformed into:

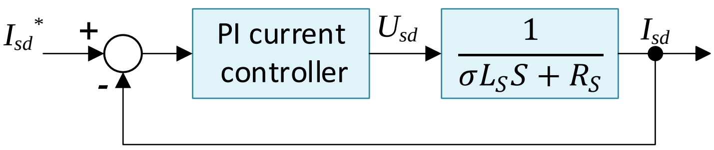

Figure 2.11 Stator current control loop (Isd and Isq).

By disregarding the time constant of the internal loop relative to the time constant of the external loop, Figure 2.10 simplifies to:

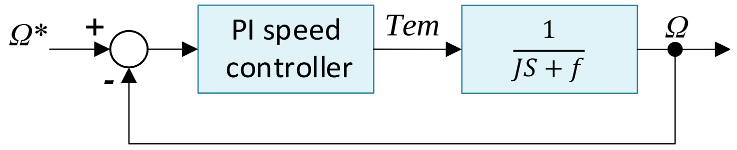

Figure 2.12 Simplified speed control loop.

T_l is considered as disturbance

2.16 Regulator Calculations

The regulation loops utilize proportional-integral (PI) controllers, chosen due to the continuous nature of the quantities being regulated. As discussed earlier, achieving ideal decoupling between the *d* and *q* axes allows us to transform our multi-variable system into two separate mono-variable systems. This enables independent analysis of the flux and torque control loops.

A Proportional Integral controller generates the control signal $u(t)$ based on the measured deviation signal $\varepsilon(t)$ from the set point, following the equation:

$$u(t) = K_p\left(\varepsilon(t) + \frac{1}{T_i}\int_0^1 \varepsilon(t)dt\right)$$

The Laplace transfer function of the controller is given by:

$$\frac{U(S)}{\varepsilon(S)} = K_p\left(1 + \frac{1}{T_i S}\right) = K_p\left(\frac{1 + T_i S}{T_i S}\right)$$

This controller has a zero that depends on T_i and a fixed pole. It can only compensate for one pole of the process, which makes it suitable for systems modeled by a first-order equation.

2.16.1 Current regulator

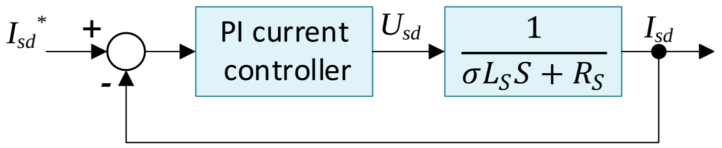

Figure 2.13 Current regulator.

The PI and the current transfer function are respectively given as

$$C_i(S) = K_{pi}\frac{T_{ii}S+1}{T_{ii}S} \tag{2.20}$$

$$I_sTF = \frac{1}{\sigma L_s S + Rs} = \frac{\frac{1}{R_s}}{\frac{\sigma L_s}{R_s}S+1} \tag{2.21}$$

with

$$T_{ii}S + 1 = \frac{\sigma L_s}{R_s}S + 1 \tag{2.22}$$

The closed loop transfer function is a first order of the following form:

$$G_{CL}(S) = \frac{\frac{K_{pi}}{R_sT_{ii}S}}{1+\frac{K_{pi}}{R_sT_{ii}S}} = \frac{1}{\frac{R_sT_{ii}}{K_{pi}}S+1} = \frac{1}{T_0S+1} \tag{2.23}$$

with to time constant fixing the behaviour in closed loop is:

$$T_{0i} = \frac{R_sT_i}{K_{pi}} \le \frac{T_{ii}}{n_i} = \frac{\sigma L_s}{R_s n_i} = \frac{1}{\omega_{cc_i}} \tag{2.24}$$

$$T_{ii} = \frac{K_{pi}}{K_{ii}} = T_0 n_i \tag{2.25}$$

If the required control n_i(Calculated according to the value of ω_{cc_i}), then the proportional gain K_{pi} can be obtained from Eq. (2.24), and the integral gain K_{ii} can be obtained from Eq. (2.25) as

$$\text{Proportional gain: } K_{pi} = \frac{R_sT_{ii}}{T_0} = \frac{R_sT_{ii}R_sn_i}{\sigma L_s} = R_sn_i \tag{2.26}$$

$$\text{Integral gain: } K_{ii} = \frac{K_{pi}}{T_0n_i} = \frac{R_sn_i}{T_0n_i} = \frac{{R_s}^2n_i}{\sigma L_s} \tag{2.27}$$

2.16.2 Speed regulator

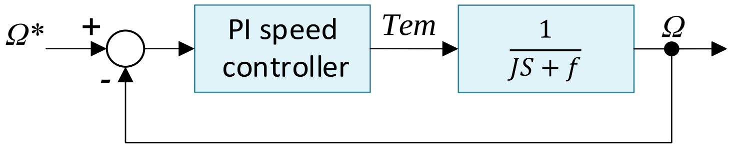

Figure 2.14 Speed control loop with a PI structure.

The PI and the speed transfer function are respectively given as

$$C_\Omega(S) = K_{p\Omega}\frac{T_{i\Omega}S+1}{T_{i\Omega}S} \tag{2.28}$$

$$\Omega TF = \frac{1}{JS+f} = \frac{\frac{1}{f}}{\frac{J}{f}S+1} \tag{2.29}$$

with

$$T_{i\Omega}S + 1 = \frac{J}{f}S + 1 \tag{2.30}$$

The open-loop transfer function $C_{\Omega OL}(S)$ is given by

$$C_{\Omega OL}(S) = \frac{K_{p\Omega}}{fT_{i\Omega}S} \tag{2.31}$$

The closed loop transfer function is a first order of the following form:

$$C_{\Omega CL}(S) = \frac{K_{p\Omega}}{fT_{i\Omega}S + K_{p\Omega}} = \frac{1}{\frac{fT_{i\Omega}}{K_{p\Omega}}S + 1} \tag{2.32}$$

with to time constant fixing the behaviour in closed loop is:

$$T_{0\Omega} = \frac{fT_{i\Omega}}{K_{p\Omega}} \leq \frac{J}{n_\Omega f} = \frac{1}{\omega_{cc_\Omega}} \tag{2.33}$$

$$T_{i\Omega} = \frac{K_{p\Omega}}{K_{i\Omega}} = T_{0\Omega}n_\Omega \tag{2.34}$$

If the required control n_Ω(Calculated according to the value of ω_{cc_Ω}), then the proportional gain $K_{p\Omega}$ can be obtained from Eq. (2.33), and the integral gain $K_{i\Omega}$ can be obtained from Eq. (2.34) as

$$\text{Proportional gain: } K_{p\Omega} = fn_\Omega \tag{2.35}$$

$$\text{Integral gain: } K_{i\Omega} = \frac{K_{p\Omega}}{T_0 n_\Omega} = \frac{f^2 n_\Omega}{J} \tag{2.36}$$

2.16.3 Flux regulator

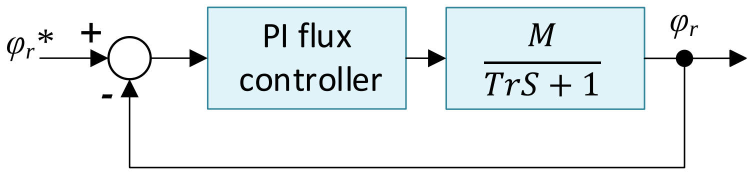

Figure 2.15 Flux control loop with a PI structure.

The PI and the flux transfer function are respectively given as

$$C_\varphi(S) = K_{p\varphi}\frac{T_{i\varphi}S + 1}{T_{i\varphi}S} \tag{2.37}$$

$$\varphi TF = \frac{\mathrm{M}}{TrS + 1} \tag{2.38}$$

with

$$T_{i\varphi}S + 1 = TrS + 1 \tag{2.39}$$

The open-loop transfer function $C_{\varphi OL}(S)$ is given by

$$C_{\varphi OL}(S) = \frac{K_{p\varphi}M}{T_{i\varphi}S} \tag{2.40}$$

The closed loop transfer function is a first order of the following form:

$$C_{\varphi CL}(S) = \frac{1}{\frac{T_{i\varphi}}{K_{p\varphi}M}S + 1} \tag{2.41}$$

with to time constant fixing the behaviour in closed loop is:

$$T_{0\varphi} = \frac{T_{i\varphi}}{K_{p\varphi}M} \leq \frac{T_{i\varphi}}{n_{\varphi}} = \frac{1}{\omega_{cc_{\varphi}}} \tag{2.42}$$

$$T_{i\varphi} = \frac{K_{p\varphi}}{K_{i\varphi}} = T_{0\varphi}n_{\varphi} \tag{2.43}$$

If the required control n_{φ}(Calculated according to the value of $\omega_{cc_{\varphi}}$) then the proportional gain $K_{p\varphi}$ can be obtained from Eq. (2.42), and the integral gain $K_{i\varphi}$ can be obtained from Eq. (2.43) as

$$\text{Proportional gain: } K_{p\varphi} = \frac{n_{\varphi}}{M} \tag{2.44}$$

$$\text{Integral gain: } K_{i\varphi} = \frac{n_{\varphi}Rr}{MLr} \tag{2.45}$$

2.16.4 Methodology for Selecting the Bandwidth in PI Control

In the realm of PI control, the speed of system response is determined by the proportional gain, Kpc, while the integral gain, Kic, plays a significant role in eliminating steady-state error. Generally, increasing these gains enhances control performance. However, caution must be exercised as excessively high gains can result in oscillations and system instability.

To determine the gains of a PI controller, it is imperative to select an appropriate bandwidth, denoted as ωcc, for the desired output control system. The selection of the bandwidth involves finding a delicate balance between achieving a fast response and avoiding instability.

The bandwidth, ωcc, of a PI controller is restricted by two factors: the switching frequency of the power electronic converter employed for the controller's output and the sampling period of the digital controller for feedback. The output control bandwidth is limited by the inability of the motor output to change at a rate faster than the switching frequency. As a general guideline, when the output is sampled twice per switching period, the maximum available bandwidth can be up to 1/10 of the switching frequency. In the case of sampling once per switching period, the maximum available bandwidth can be up to 1/20 of the switching frequency. It is advisable to restrict the bandwidth to 1/25 of the sampling frequency in the latter scenario [1].

These considerations ensure a suitable trade-off between control performance and system stability within the PI controller. The selection of appropriate values for Kpc, Kic, and ωcc is crucial to achieving the desired control performance in motor control systems.

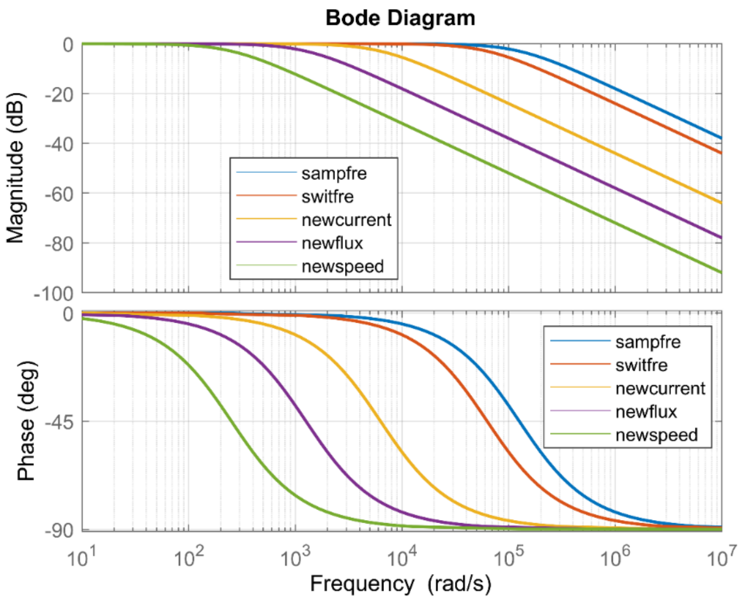

Figure 2.16 Bode diagram for system frequency.

In the context of selecting the bandwidth for PI control, the diagram provides valuable insights into the frequency domain response of the system elements. The diagram reveals the gain cross-over frequency, ω_{cc}, where a change in direction occurs at -45 degrees, which serves as a determining factor for the bandwidth.

Considering the specific parameters of the system, we have a sampling time of 20000Hz, which is twice as large as the switching time of 1000Hz. As a result, the bandwidth of the current at 1000Hz is ten times smaller, while the bandwidth of the flux at 200Hz is five times smaller than its subsequent value. Furthermore, the speed exhibits a bandwidth that is 5 times smaller than the flux at 40Hz. These relationships and variations in bandwidth values provide important insights into the behavior of the system elements within the specified frequency ranges.

2.17 Simulation of the vector control of the IM (direct and Indirect)

In this research, we conducted a simulation of an IM operating with a PWM voltage inverter and being controlled by vectors. The simulation encompassed two different modes of operation: one without any load and another with a load.

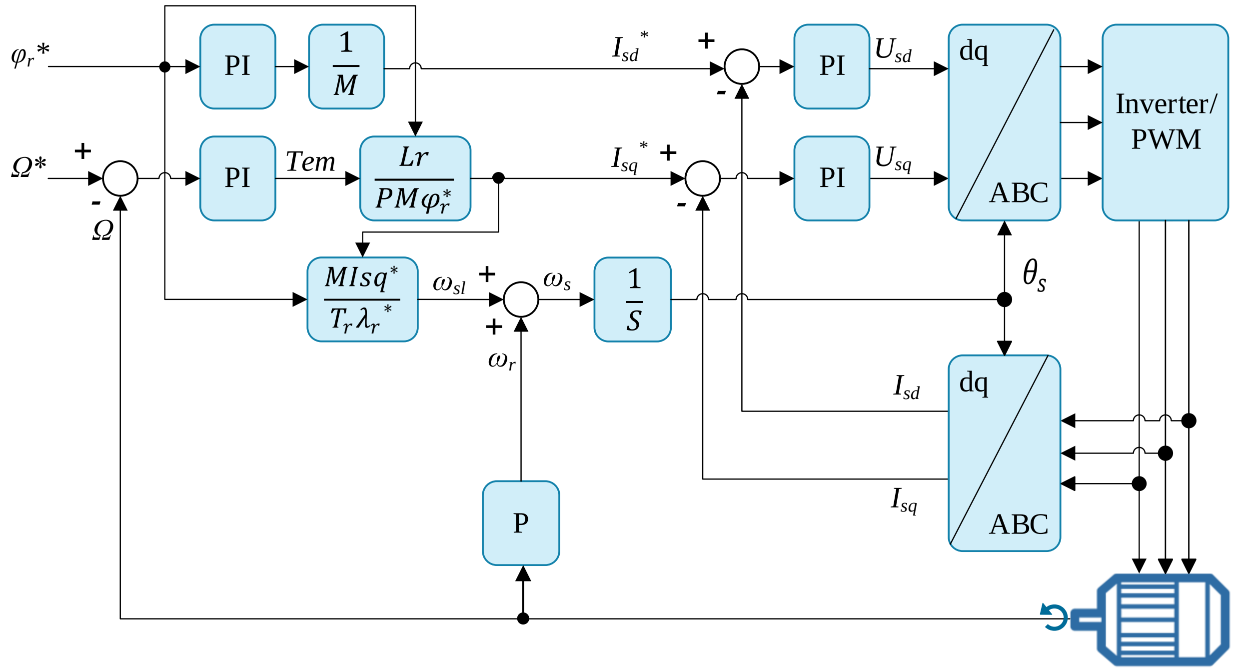

Figure 2.18 Indirect Field-Oriented Control (FOC) implementation for the induction motor (IM).

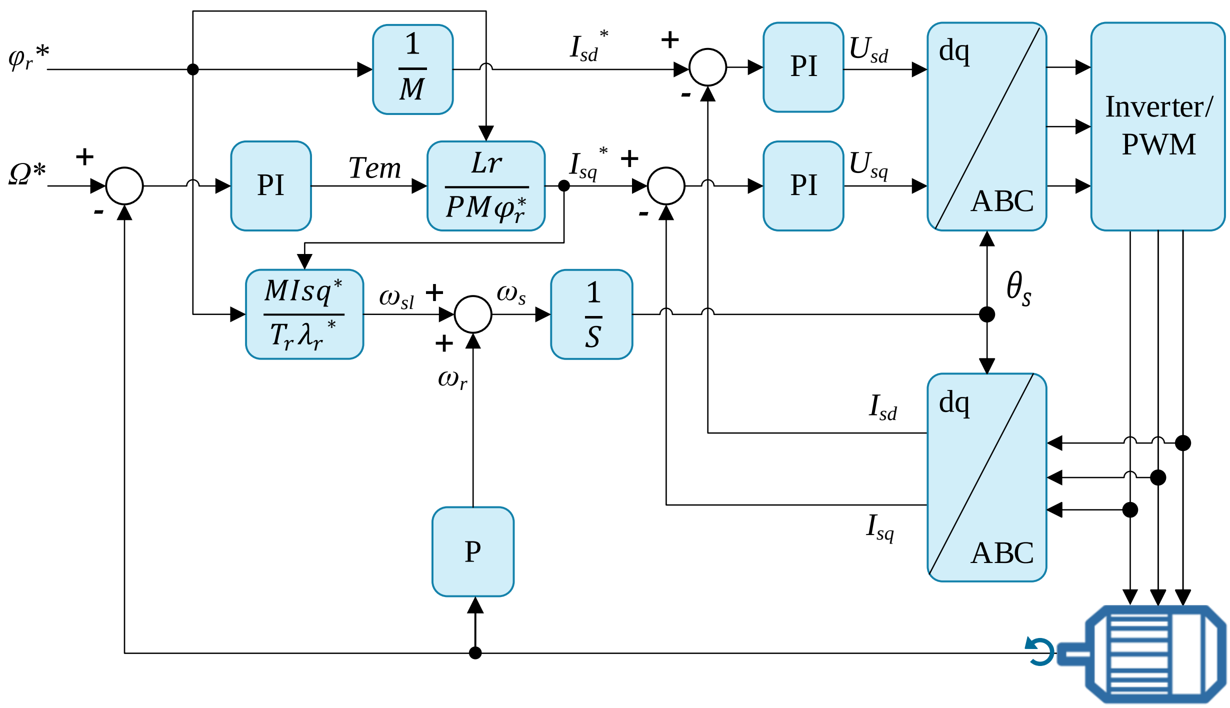

Figure 2.19 Direct Field-Oriented Control (FOC) implementation for the induction motor (IM).

2.18 Simulation results

In this section, we will conduct a simulation of the direct vector control and indirect vector control of an induction motor (IM) powered by a two-level inverter. It is important to note that the simulation is performed under the specified conditions, which include a reference flux of 1Wb and a reference speed that varies from 0 to 100 rad/s. Additionally, a load torque of 10 Nm is applied at different time intervals during the simulation.

Indirect FOC results

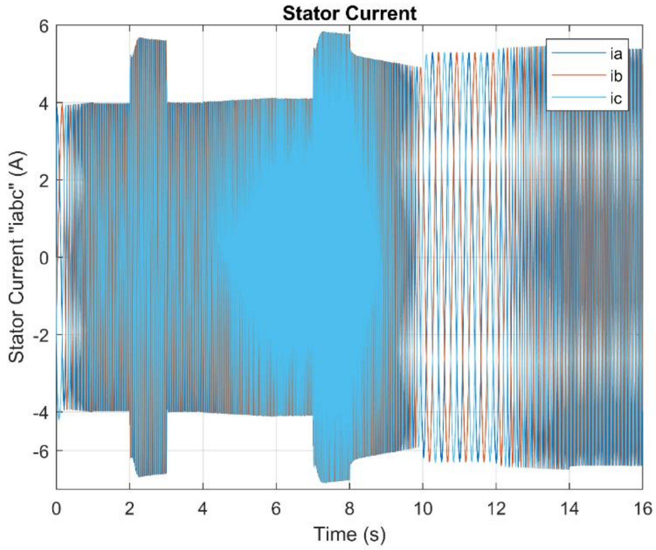

Figure.2.20 Diagram of current simulation over time.

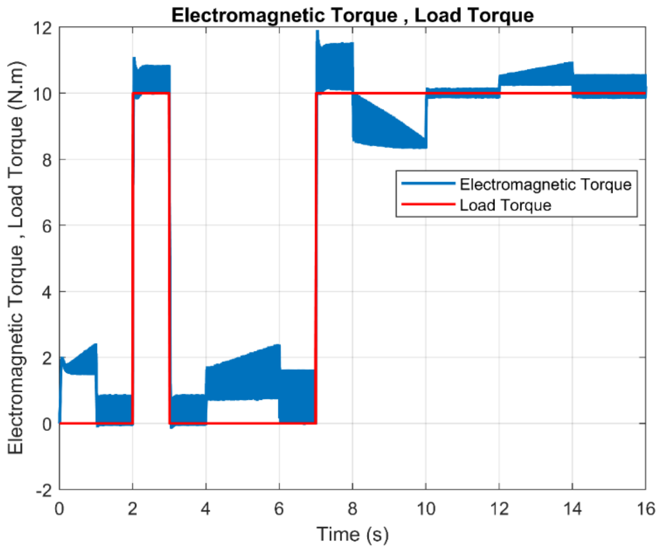

Figure 2.21 Diagram of electromagnetic torque simulation over time.

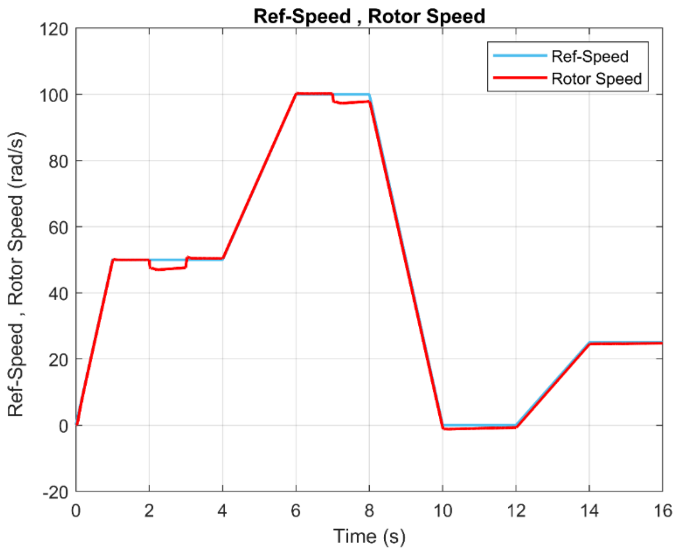

Figure 2.22 Diagram of rotor speed simulation over time.

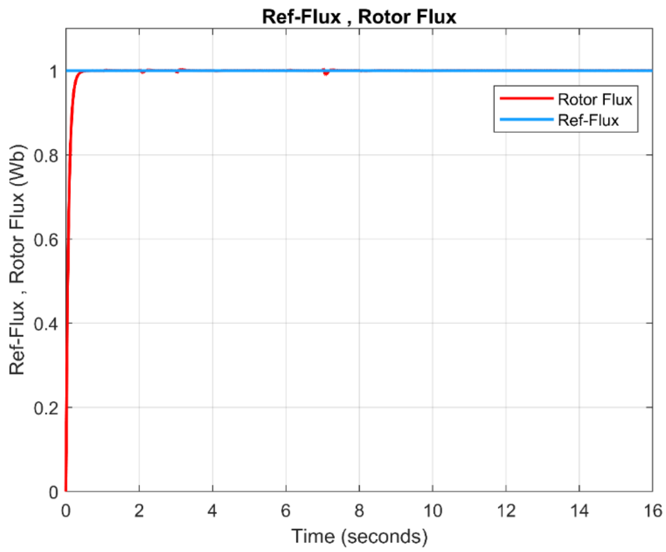

Figure 2.23 Diagram of rotor flux simulation over time.

The machine initiates its operation without any load, starting from time t = 0 with a speed of 0 rad/s. It smoothly increases the speed, following the reference, until t = 1s, reaching 50 rad/s. As a result, the machine generates a torque of 2 N.m, and a momentary current is generated during startup to enable the machine to develop the required torque. Subsequently, the machine stabilizes at a current of 4 A.

Once the speed stabilizes at 50 rad/s, the torque is cancelled. However, at t = 2s, a load torque of 10 N.m is applied. It is observed that both the torque and the electric current increase by the value of the applied load torque, specifically 10 Nm and 1.7 A respectively, in order to meet the load torque requirement. The speed experiences a slight decrease but returns to the reference value.

Between t = 8 and t = 10, the speed gradually decreases from 100 rad/s to 0 rad/s, aligning with the reference. During this period, the torque decreases to 8.5 Nm while maintaining the same value of the applied load torque of 10 N.m, resulting in a "braking" effect. While the flux initially shows a gradual increase, it eventually aligns with the reference value. However, the absence of a controller causes the flux to fluctuate whenever there is a change in velocity.

Direct FOC results

In this section, we conducted a simulation of direct control on an IM transmission (asynchronous machine system) powered by a two-level inverter. The simulation was carried out under specific conditions, including a reference flux of 1*Wb* and a velocity that will be modeled according to the table provided. The following tests were performed to evaluate the performance of the system:

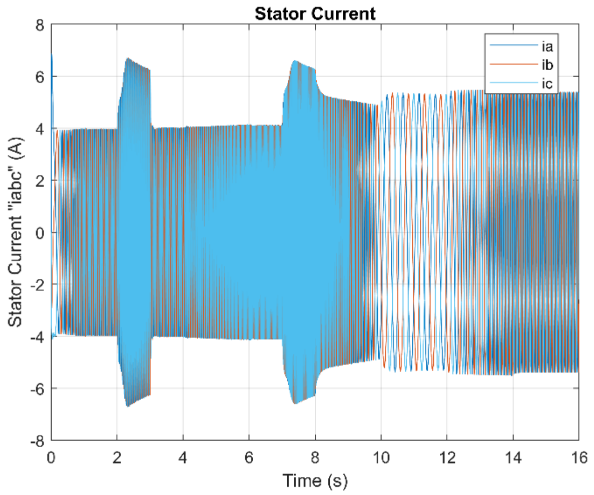

Figure 2.24 Diagram of current simulation over time.

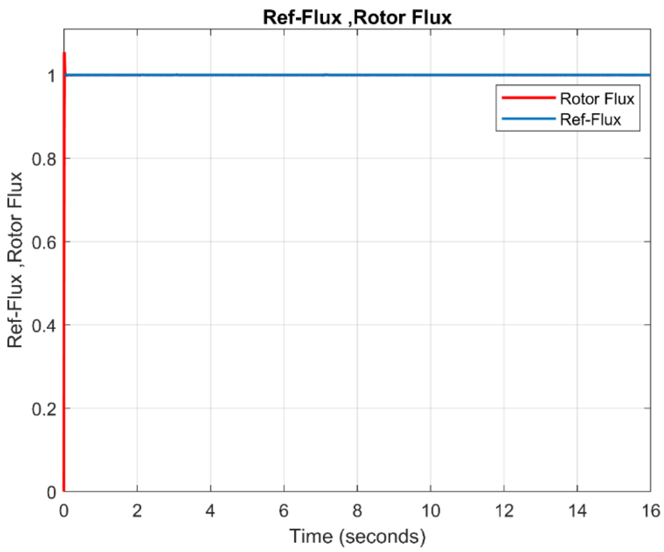

Figure 2.25 Diagram of rotor flux simulation over time.

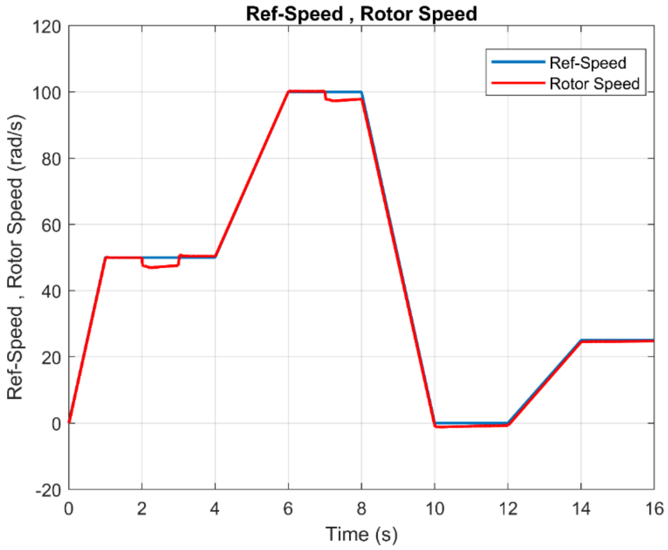

Figure 2.26 Diagram of rotor speed simulation over time.

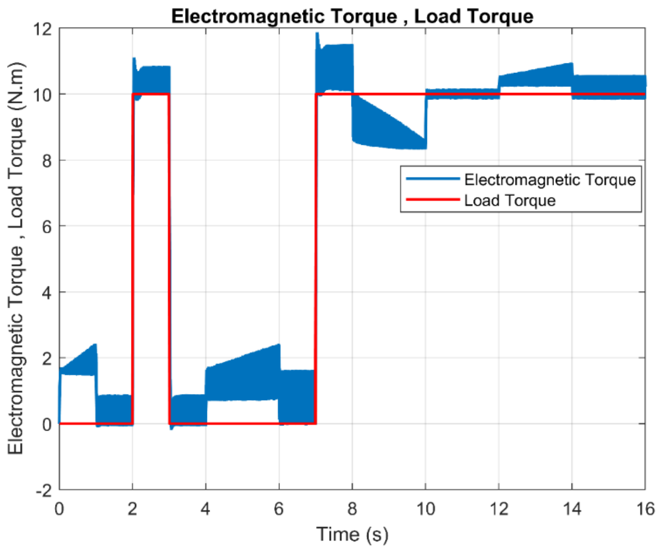

Figure 2.27 Diagram of electromagnetic torque simulation over time.

The machine initiates its operation without any load, starting from time t = 0 and a speed of 0 rad/s. In a smooth and incremental manner, the speed gradually increases until t = 1s, reaching a value of 50 rad/s, accurately following the reference speed. Consequently, the machine generates a torque of 2 N.m, and during the startup phase, a momentary current is generated to ensure the machine produces the required torque. Subsequently, the machine stabilizes at a current of 4.5 A.

Following the stabilization of the speed at 50 rad/s, the torque is nullified. However, at t = 2s, a load torque of 10 Nm is applied. It is observed that both the torque and the electric current increase by the value of the applied load torque, namely 10 Nm and 1.5 A respectively, in order to meet the load torque requirement. The speed experiences a slight decrease but then returns to the reference speed.

Between t = 8 and t = 10, the speed decreases from 100 rad/s to 0 rad/s, aligning with the reference speed. During this period, the torque decreases to 8.5 Nm while maintaining the same value of the applied load torque, resulting in a "braking" effect. It is noteworthy that during the initial phase, the flux briefly overshoots, but unlike in indirect control, it consistently aligns with the reference throughout the entire simulation period. This precise control over the flux is attributed to the PI controller.

In terms of performance, the direct vector control technique outperformed the indirect vector control technique, exhibiting a faster response time..

2. 20 Conclusion

In summary, the adoption of sophisticated control techniques like Field-Oriented Control (FOC) has demonstrated significant benefits in managing current, speed, and torque compared to conventional approaches such as Scalar control. FOC facilitates more accurate and effective regulation of the induction motor, resulting in enhanced performance and energy utilization.

Through the utilization of FOC, the motor system can attain superior current regulation by minimizing irregularities and ensuring smoother operation. Moreover, FOC improves speed control, enabling better alignment with the desired speed reference and enhancing the overall dynamics of the system. Furthermore, FOC optimizes torque generation, resulting in higher torque density and improved overall efficiency of the motor.

Chapter 3

Control of IM using Backstepping Technique

3.1 Introduction

Backstepping control, a prominent technique in the realm of nonlinear control theory, addresses the limitations posed by imperfect process models that hinder the full linearization of systems through feedback control. Unlike their perfectly linearizable counterparts, these systems possess partial linearizability due to inherent imperfections in their process models. Over the past two decades, substantial advancements have been made in nonlinear control theory to overcome these challenges, resulting in the development of various techniques employed in the design and implementation phases of control models for nonlinear systems. Among these techniques, the Backstepping Theory stands out as a well-established approach that employs the recursive design of control laws based on the principles of Lyapunov theory. Presently, nonlinear systems are characterized by enhanced structure and development, owing in part to the application of these techniques.

3.2 Lyapunov's Theory and Stability

In order for a controlled system to work properly, it needs to eventually reach a specific state. This can be described as the desired equilibrium. When analyzing a dynamic system, stability is the most important aspect to look into. Stability can be understood in different ways in control theory, like the stability of a specific point or how the input and output are connected. The study of stability has made great progress, especially with the introduction of Lyapunov's stability theory, which helps determine the stability of linear dynamic models. [11]

3.2.1 Stability in the sense of Lyapunov

The two Lyapunov methods hold significant importance as analytical techniques. The first method, referred to as the linearization method, focuses on assessing the stability of a nonlinear system in the vicinity of its equilibrium point by utilizing a linear approximation. By employing tools from linear control systems, this approach enables effective analysis. The second method, more comprehensive in nature, utilizes the energy principle to examine stability. According to this method, a physical system is considered stable if its total mechanical energy decreases over time. Lyapunov developed a function with properties akin to energy, facilitating more convenient stability analysis [11].

A. Lyapunov's first method

Lyapunov's first method, which is also called the local stability theorem, enables us to decide on the linearization of a system's dynamics around a point of equilibrium. This theorem gives theoretical validity to the linearization technique and states the following:

- If the linearized system is asymptotically stable, the system is also asymptotically stable.
- If the linearized system is unstable, the system is also unstable.
- If the linearized system is stable without being asymptotically stable, we cannot make a definitive statement. This is the critical case of Lyapunov, and the stability or instability, in this case, depends on the higher-order terms that were neglected in the approximation.

B. Lyapunov's second method

Lyapunov's approach is to use a scalar function V, also known as an Energy function, to investigate the stability of the system by analyzing its changes (sign of V) along the system's trajectory.

3.2.2 Lyapunov candidate function

Lyapunov's candidate is a function $V(x)$ which has two essential properties:

- There are two qualities that are important to consider when analysing the stability of an equilibrium point using Lyapunov's method. The first quality is the extremum of the function at the equilibrium point, which can be a maximum or a minimum. The equilibrium point is considered stable if this extremum is a minimum. To ensure the presence of a minimum at the equilibrium point, the function must be positive for any value other than the origin and can only be zero at the origin.
- The second characteristic of Lyapunov's candidate function is that it tends to decrease or stay constant during the evolution of a stable system. Therefore, for the function to be considered a Lyapunov candidate, its derivative must also be negative [11].

$$\dot{V}(x) = \left(\frac{dV}{dx}\right)^T f(x) < 0 \tag{3.1}$$

3.3 Backstepping control design

3.3.1 Principle

In the past years, there have been significant advancements in the area of nonlinear system control, and one of the latest developments is the backstepping technique. This technique provides a systematic synthesis method for nonlinear systems that have a triangular shape. The technique decomposes the entire control system, which is typically high order and multivariable, into a cascade of first-order control subsystems. A virtual control law is then calculated for each subsystem.

In the past few years, significant progress has been made in the field of controlling nonlinear systems, and the backstepping technique is one of the recent developments in this area. It suggests a systematic synthesis method designed for the class of nonlinear systems that have a triangular shape. This technique involves decomposing the entire control system, which is usually multivariable (MIMO) and high order, into a cascade of first-order control subsystems. For each subsystem, a virtual control law is calculated, which will be used as a reference for the next subsystem until the control law for the entire system is obtained (as shown in Figure 3.1). Moreover, this technique has the advantage of holding the useful nonlinearities for the control's performance and robustness, unlike linearization methods. The determination of the control laws resulting from this approach is based on the use of Control Lyapunov Functions (CLF) [4].

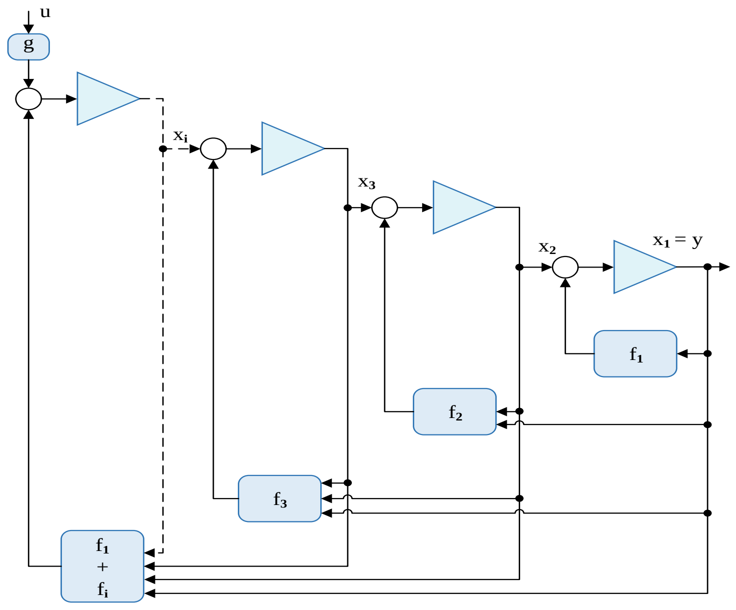

Figure 3.1 General procedure of backstepping control design.

3.3.2 General method of recursive synthesis by Backstepping

The recursive synthesis technique known as Backstepping is a widely used approach in engineering and control systems. It provides a general method for systematically designing controllers that can handle complex and nonlinear systems. By breaking down the control problem into a series of smaller, more manageable sub-problems, Backstepping enables engineers to progressively build a controller that can achieve desired system behavior. This approach is particularly valuable when dealing with systems that exhibit nonlinearities, uncertainties, or disturbances. By employing recursive strategies and feedback loops, Backstepping allows for the synthesis of controllers that can effectively handle a wide range of challenging control tasks. This approach is suitable for systems with a triangular structure, as illustrated in the diagram below:

$$\begin{aligned} \dot{X}_1 &= f_1(x_1) + g_0(x_1)x_2 \\ \dot{X}_2 &= f_2(x_1, x_2) + g_1(x_1, x_2)x_3 \\ &\vdots \\ \dot{X}_n &= f_n(x_1, \cdots, x_n) + g_n(x_1, \cdots, x_n)u \end{aligned} \tag{3.2}$$

with :

$$x = [x_1, x_2 \cdots, x_n]^T \in R^n, u \in R$$

To demonstrate the recursive process of the Backstepping technique, let us assume that the desired reference signal for the output $y = x_1$ is y_{ref}. Since the system is of order n, the approach will involve *n* steps to implement.

Step 1

The Backstepping method is initiated by considering the first equation of the system (3.2), and treating x_2 as an intermediate virtual command. The first reference value is denoted as:

$$(x_1)_d = \alpha_0 = y_{ref} \tag{3.3}$$

This leads to the following regulation error:

$$e_1 = x_1 - \alpha_0 \tag{3.4}$$

Thus, the derivative of the first desired reference can be expressed as:

$$\begin{aligned} \dot{e}_1 &= \dot{x}_1 - \dot{\alpha}_0 \\ &= f_1(x_1) + g_0(x_1)x_2 - \dot{\alpha}_0 \end{aligned} \tag{3.5}$$

The first step in analyzing such a system is to create the Lyapunov function V_1, which takes the form of a quadratic equation.

$$V_1 = \frac{1}{2}e_1^2 \tag{3.6}$$

The time derivative of V_1 is given by:

$$\begin{aligned} \dot{V}_1 &= e_1\dot{e}_1 \\ &= e_1[f_1(x_1) + g_0(x_1)x_2 - \dot{\alpha}_0] \end{aligned} \tag{3.7}$$

Choosing the appropriate value of x can make $\dot{V}_1$ negative, ensuring stability for the dynamics of equation (3.5). In order to achieve this, we can set x_2 equal to α, which satisfies the condition:

$$f_1(x_1) + g_0(x_1)x_2 - \dot{\alpha}_1 = -k_1e_1 \tag{3.8}$$

where $k_1 > 0$ is a design constant.

Therefore, the expression for the control law of system (3.5) is:

$$\alpha_1 = \frac{1}{g_0(x_1)}[-k_1e_1 + \dot{\alpha}_0 - f_1(x_1)] \tag{3.9}$$

which implies

$$\dot{V}_1 = -k_1e_1^2 \leq 0 \tag{3.10}$$

Step 2

A new desired reference will now be chosen as the control variable for the previous subsystem (3.5).

$$(x_2)_d = \alpha_1 \tag{3.11}$$

The resulting regulation error is:

$$e_2 = x_2 - \alpha_1 \tag{3.12}$$

$$\begin{aligned} \dot{e}_2 &= \dot{x}_2 - \dot{\alpha}_1 \\ &= f_2(x_1, x_2) + g_1(x_1, x_2)x_3 - \dot{\alpha}_1 \end{aligned} \tag{3.13}$$

It derives it:

The extended Lyapunov function for the system (3.13) is given by:

$$\begin{aligned} V_2 &= V_1 + \frac{1}{2}e_2^2 \\ &= \frac{1}{2}[e_1^2 + e_2^2] \end{aligned} \tag{3.14}$$

whose derivative is:

$$\begin{aligned} \dot{V}_2 &= \dot{V}_1 + e_2\dot{e}_2 \\ &= -k_1e_1^2 + e_2[f_2(x_1, x_2) + g_1(x_1, x_2)x_3 - \dot{\alpha}_1] \end{aligned} \tag{3.15}$$

The choice of (x_3) which stabilizes the dynamics of the system (3.13) and will make V_2 negative is:

$x_3 = \alpha$ such that:

$$f_2(x_1, x_2) + g_1(x_1, x_2)x_3 - \dot{\alpha}_1 = -k_2e_2 \tag{3.16}$$

Where $\mathrm{k}_2 > 0$ is a design constant:

Therefore, the control law for system (3.13) can be expressed as:

$$\alpha_1 = \frac{1}{g_1(x_1, x_2)}[-k_2e_2 + \dot{\alpha}_1 - f_2(x_1, x_2)] \tag{3.17}$$

with:

$$\dot{\alpha}_1 = \frac{g_0(x_1)[-k_1\dot{e}_1 + \ddot{\alpha}_0 - \dot{f}_1(x_1)] - [-k_1e_1 + \dot{\alpha}_0 - f_1(x_1)]\dot{g}_0(x_1)}{g_0^2(x_1)} \tag{3.18}$$

This choice leads to:

$$\dot{V}_2 = -k_1e_1^2 - k_2e_2^2 \leq 0 \tag{3.19}$$

Step n

In a similar manner, for this step, the new reference to be followed will be:

$$(x_n)_d = \alpha_{n-1} \tag{3.20}$$

hence the regulation error:

$$e_n = x_n - \alpha_{n-1} \tag{3.21}$$

Its derivative is:

$$\begin{aligned} \dot{e}_n &= \dot{x}_n - \dot{\alpha}_{n-1} \\ &= f_n(x_1, \cdots, x_n) + g_n(x_1, \cdots, x_n)u - \dot{\alpha}_{n-1} \end{aligned} \tag{3.22}$$

For the system (3.22), the extended Lyapunov function is:

$$\begin{aligned} V_n &= V_1 + V_2 + \cdots + \frac{1}{2}e_n^2 \\ &= \frac{1}{2}[e_1^2 + \cdots e_n^2] \end{aligned} \tag{3.23}$$

Its derivative is:

$$\begin{aligned} \dot{V}_n &= \dot{V}_1 + \cdots + e_n\dot{e}_n \\ &= -k_1e_1^2 + \cdots + e_n[f_n(x_1, \cdots, x_n) + g_n(x_1, \cdots x_n)u - \dot{\alpha}_{n-1}] \end{aligned} \tag{3.24}$$

The control law derived in the final step should meet the following requirements:

$$f_n(x_1, \cdots, x_n) + g_n(x_1, \cdots, x_n)u - \dot{\alpha}_{n-1} = -k_ne_n \tag{3.25}$$

Or $k_n>0$ is a constant conception.

Therefore, the control law for the complete system can be expressed as:

$$u_1 = \frac{1}{g_n(x_1, \cdots x_n)}[-k_ne_n + \dot{\alpha}_{n-1} - f_n(x_1, \cdots x_n)] \tag{3.26}$$

This ensures that the time derivative of the extended Lyapunov function is negative:

$$\dot{V}_n = -k_1e_1^2 - \cdots - k_ne_n^2 \leq 0 \tag{3.27}$$

3.3.3 Application of the Backstepping techniquer for Controlling the IM

The application of the Backstepping technique to the IM is based on the following steps:

- We will compute the initial virtual control input for a subsystem by using the error signal and the adaptation dynamics, which will serve as a reference signal for the subsequent state in the second stage. $e_1 = (y_{ref} - y)$.
- find a Lyapunov function for which the derivative is negative.
- Repeat the previous steps until reaching the nth stage, which corresponds to the order of the system. At this stage, we will have generated the control law that ensures the overall stability of the system, and we will apply it to

$$\begin{aligned}
\frac{di_{sd}}{dt} &= -\gamma i_{sd} + \omega_s i_{sq} + \frac{MR_r}{\sigma L_s L_r}\phi_{rd} + \frac{1}{\sigma L_s}U_{sd} \\
\frac{di_{sq}}{dt} &= -\gamma i_{sq} - \omega_s i_{sd} - \frac{M}{\sigma L_s L_r}\omega_m \phi_{rd} + \frac{1}{\sigma L_s}U_{sq} \\
\frac{d\phi_{rd}}{dt} &= -\frac{\phi_{rd}}{T_r} + \frac{M}{T_r}i_{sd} \\
\frac{d\Omega}{dt} &= \frac{PM}{JL_r}\phi_{rd} i_{sq} - \frac{T_l}{J} - \frac{f}{J}\Omega
\end{aligned} \tag{3.28}$$

with:

$$\gamma = \left(R_s + \frac{M^2 R_r}{L_r^2}\right)\frac{1}{\sigma L_s}$$

$$\sigma = 1 - \frac{M^2}{L_s L_r}$$

$u = [U_{sd} \quad U_{sq}]^T$: The entrance to the induction machine.

$y = x_1 = [\Omega \quad \phi_r]^T$:Its controlled output.

$x_2 = [I_{sd} \quad I_{sq}]^T$: Stator current vector.

$x = [x_1 \quad x_2]$: The state vector.

Our goal is to force the output $y = x_1$ to follow their references, $\Omega_{ref}, \phi_{r_{ref}}$ respectively.

The first step

The aim of this step is to eliminate the speed and flux regulators. The errors e_1 and e_2 are defined, representing the difference between the actual values of the speed and the flux magnitude, respectively, and their respective reference values. The tracking errors for the rotor speed and flux are defined as:

$$e_1 = \Omega_{ref} - \Omega$$
$$e_2 = \phi_{r_{ref}} - \phi_r \tag{3.29}$$

Let us consider the positive definite energy function *V1* given by:

$$V_1 = \frac{1}{2}e_1^2 + \frac{1}{2}e_2^2 \tag{3.30}$$

Its derivative is:

$$\dot{V}_1 = e_1\dot{e}_1 + e_2\dot{e}_2 = e_1(\dot{\Omega}_{ref} - \dot{\Omega}) + e_2\left(\dot{\phi}_{r_{ref}} - \dot{\phi}_r\right) \tag{3.31}$$

$$\dot{V}_1 = e_1\left(\dot{\Omega}_{ref} - \frac{PM}{JL_r}\phi_r I_{sq} + \frac{f}{J}\Omega + \frac{1}{J}T_l\right) + e_2\left(\dot{\phi}_{r_{ref}} - \frac{M}{\tau_r}I_{sd} + \frac{1}{\tau_r}\phi_r\right) \tag{3.32}$$

If we substitute I_{sd} with $I_{sd_{ref}}$ and I_{sq} with $I_{sq_{ref}}$, then the dynamics of the energy function can be expressed as:

$$\dot{V}_1 = e_1\left(\dot{\Omega}_{ref} - \frac{PM}{JL_r}\phi_r I_{sq_{ref}} + \frac{f}{J}\Omega + \frac{1}{J}T_l\right) + e_2\left(\dot{\phi}_{r_{ref}} - \frac{M}{\tau_r}I_{sd_{ref}} + \frac{1}{\tau_r}\phi_r\right) \tag{3.33}$$

To make $\dot{V}_1$ negative, we make a suitable choice of the new virtual inputs $I_{sd_{ref}}$ and $I_{sq_{ref}}$ In the following way:

$$I_{sd_{ref}} = \frac{JL_r}{PM\phi_r}\left(K_1e_1 + \dot{\Omega}_{ref} + \frac{f}{J}\Omega + \frac{1}{J}T_l\right)$$
$$I_{sq_{ref}} = \frac{\tau_r}{M}\left(K_2e_2 + \dot{\phi}_{r_{ref}} + \frac{1}{\tau_r}\phi_r\right) \tag{3.34}$$

This means that *K1* and *K2* are constants that are positive without any possibility of being zero or negative.

Figures (3.2) and (3.3) represent the block diagrams for calculating the currents $I_{sd_{ref}}$ and $I_{sq_{ref}}$ respectively.

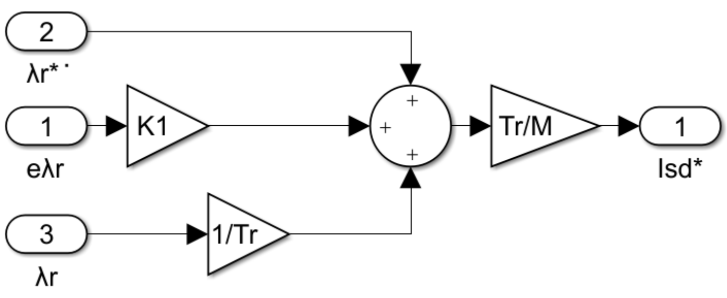

Figure 3.2 Block diagram for calculating (I_{sdref})

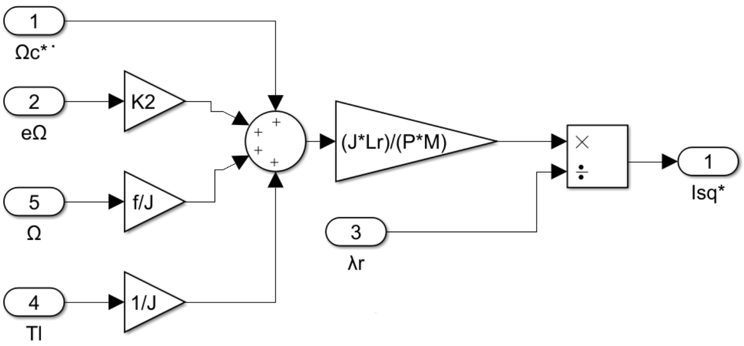

Figure 3.3 Block diagram for calculating the (I_{sqref}).

The second step

We define the Lyapunov function candidate *V(x)* for our system, with the purpose of calculating the control voltages. Other errors related to the stator current components and their references are defined.

$$V(x) = V_1(x) + \frac{1}{2}e_3^2 + \frac{1}{2}e_4^2 \tag{3.35}$$

Such as:

$$\begin{aligned} e_3 &= I_{sq_{ref}} - I_{sq} \\ e_4 &= I_{sd_{ref}} - I_{sd} \end{aligned} \tag{3.36}$$

Therefore, the derivative of the candidate Lyapunov function will be:

$$\dot{V}(x) = \dot{V}_1(x) + e_3\dot{e}_3 + e_4\dot{e}_4 = \dot{V}_1(x) + e_3\left(\dot{I}_{sq_{ref}} - \dot{I}_{sq}\right) + e_4\left(\dot{I}_{sd_{ref}} - \dot{I}_{sd}\right) \tag{3.37}$$

$$\begin{aligned} \dot{V}(x) = \dot{V}_1(x) &+ e_3\left(\dot{I}_{sq_{ref}} + \omega_s I_{sd} + \gamma I_{sq} + \frac{PM}{\sigma L_s L_r}\Omega\phi_r - \frac{1}{\sigma L_s}U_{sq}\right) \\ &+ e_4\left(\dot{I}_{sd_{ref}} + \gamma I_{sd} - \omega_s I_{sq} - \frac{M}{\sigma L_s L_r \tau_r}\phi_r - \frac{1}{\sigma L_s}U_{sd}\right) \end{aligned} \tag{3.38}$$

The control law we select is:

$$\begin{aligned} U_{sq_{ref}} &= \sigma L_s(K_3 e_3 + \dot{I}_{sq_{ref}} + \omega_s I_{sd} + \gamma I_{sq} + \frac{PM}{\sigma L_s L_r}\Omega\phi_r) \\ U_{sd_{ref}} &= \sigma L_s(K_4 e_4 + \dot{I}_{sd_{ref}} + \gamma I_{sd} - \omega_s I_{sq} - \frac{M}{\sigma L_s L_r \tau_r}\phi_r) \end{aligned} \tag{3.39}$$

K_4 and K_3 are strictly positive constants.

The diagrams depicted in figures (3.5) and (3.4) illustrate the process of determining the currents $U_{sd_{ref}}$ and $U_{sq_{ref}}$ correspondingly.

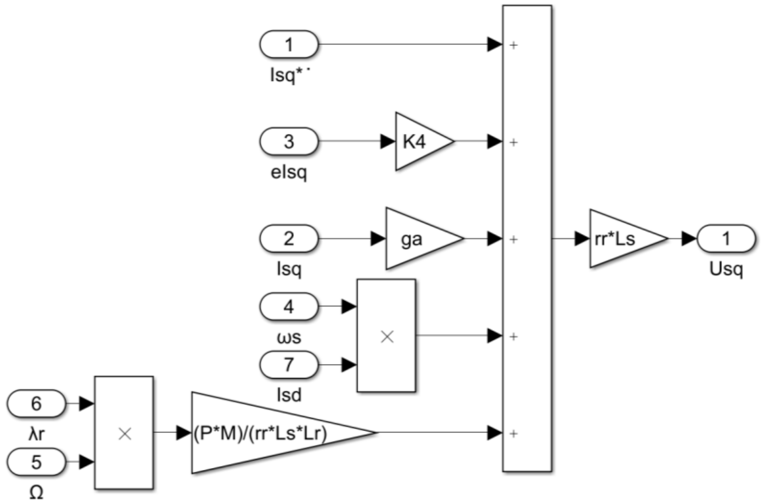

Figure 3.4 Block diagram for calculate U_{sqref}.

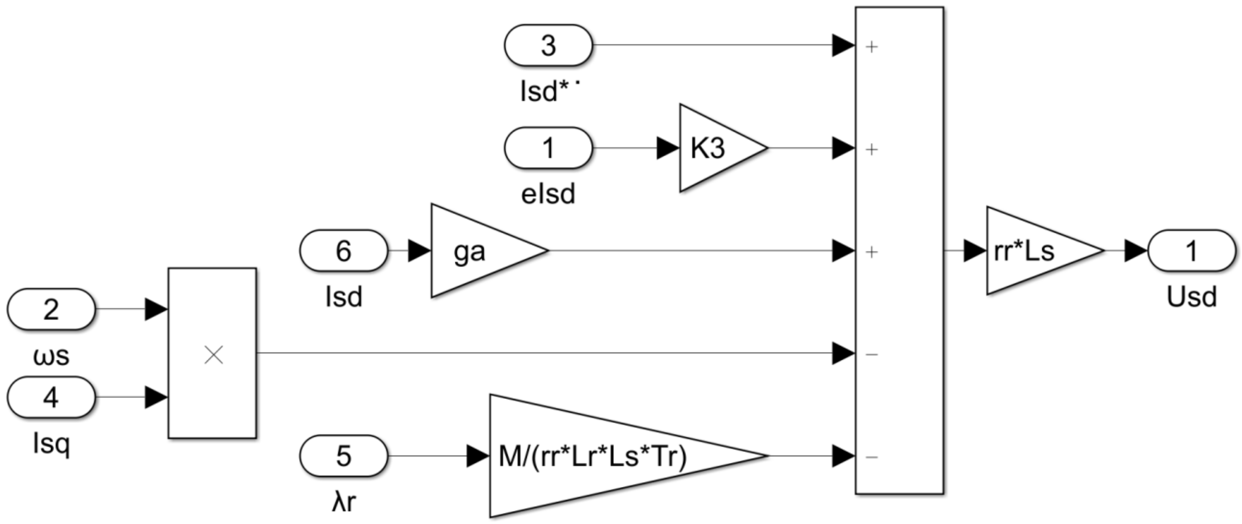

Figure 3.5 Block diagram for calculate U_{sdref}.

The negative derivative of the Lyapunov function implies stability of the machine under the Backstepping control.

3.4 Simulation of Backstepping control of the IM

In this study, we simulated an induction motor that runs on a PWM voltage inverter and is under Backstepping control. The simulation was carried out in two operating modes: with no load and with a load.

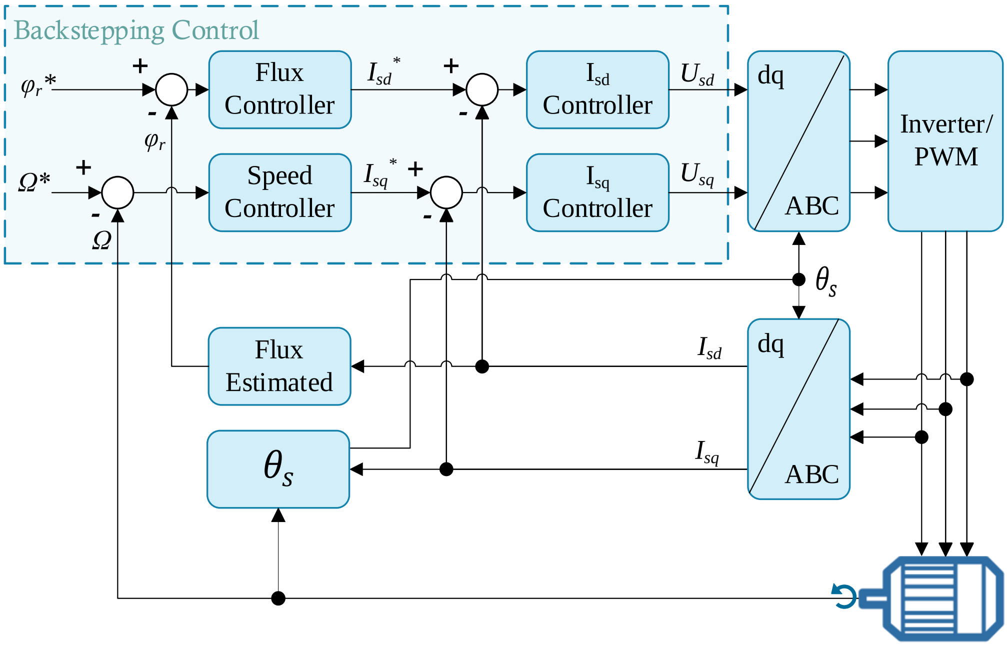

Figure 3.6 Diagram depicting the block structure of the Backstepping control applied to the induction motor (IM).

3.4.1. Simulation results

In this section, we will simulate the direct vector control based on backstepping for an induction motor (IM) using a two-level inverter. The simulation is performed under the following conditions:

- Reference flux of 1Wb
- Reference speed ranging from 0 to 100 rad/s
- Load torque of 10 Nm applied at different time intervals

The results of the simulation will be used to compare the performance of the two control methods.

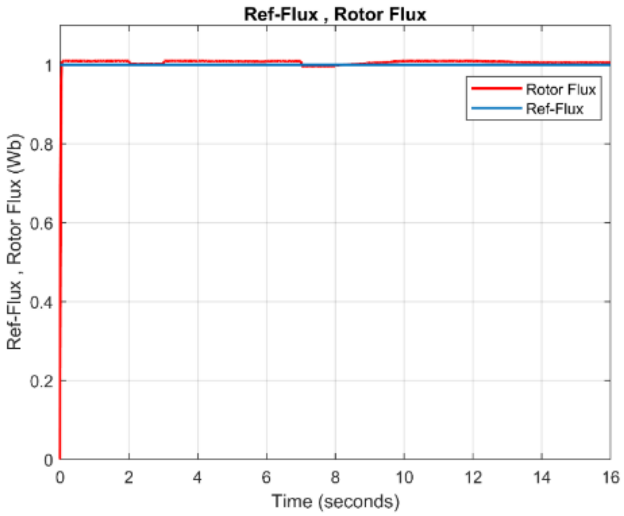

Figure 3.8 Diagram of stator flux simulation over time.

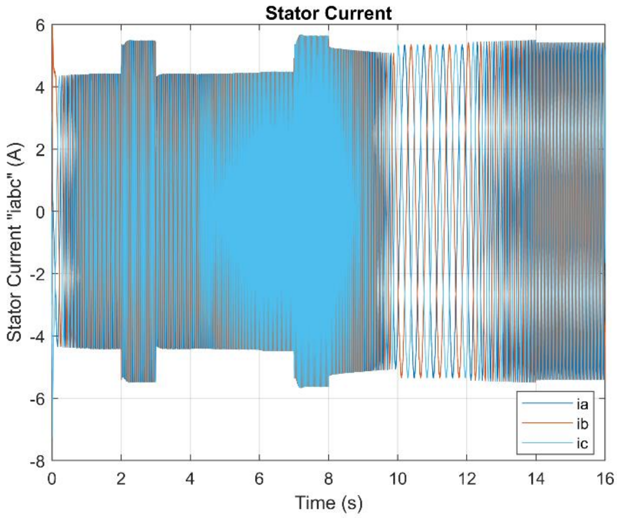

Figure 3.7 Diagram of stator current simulation.

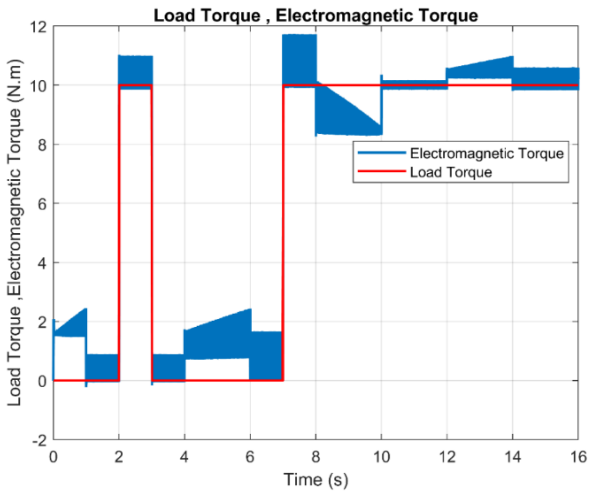

Figure 3.10 Diagram of electromagnetic torque simulation over time.

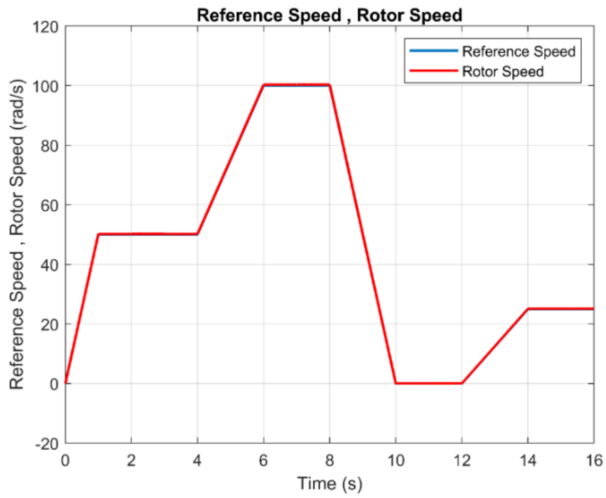

Figure 3.9 Diagram of rotor speed simulation over time.

The machine initiates its operation at t = 0 with no load, starting from a speed value of 0 rad/s. It gradually increases its speed in a smooth manner until t = 1s, reaching a speed of 50 rad/s, following the reference accurately. As a result, the machine generates a torque of 2 N.m, and a momentary current of 26 A is produced during motor startup to enable the machine to generate the required torque. Subsequently, the machine stabilizes at a current of 4.5 A.

At t = 2s, a load torque of T_l = 10 Nm is applied. It is observed that both the torque and the electric current increase by the value of the applied load torque, i.e., 10 Nm and 1.5 A respectively, in order to meet the load torque requirement.

Between t = 8 and t = 10, the speed decreases from 100 rad/s to 0 rad/s, matching the reference speed. During this period, the torque decreases to 8.5 Nm while maintaining the same value of the applied load torque, resulting in a "braking" effect.

One note that the backstepping control technique exhibited significantly superior performance compared to the other control techniques investigated in this research, regardless of the specific circumstances. These superior results were particularly noticeable during transient stages and when a load was introduced.

3.5 Conclusion

In conclusion, this chapter has introduced the concept of stability in the sense of Lyapunov and discussed the direct method, proposed by Lyapunov. Additionally, the Backstepping control technique, which is based on the direct method of Lyapunov, was presented as a systematic and straightforward approach for synthesizing control laws and ensuring the stability of a system.

The application of the Backstepping control technique to the asynchronous machine demonstrated its effectiveness in stabilizing the machine. By carefully selecting an appropriate Lyapunov function and following a step-by-step process, the control laws were established to maintain stability throughout the operation of the machine.

Furthermore, based on the obtained results, it can be concluded that the Backstepping control technique outperformed other classical control techniques, particularly during transient stages and when subjected to load conditions. This suggests that the Backstepping control technique offers superior performance and robustness in controlling the induction motor, making it a favorable choice for such applications.

Conclusion general

In conclusion, the techniques discussed in this thesis, including scalar control, field-oriented control (FOC), and Backstepping control, have shown their significance and effectiveness in the context of induction motor control.

The first chapter focused on the modelling of the motor using the Park model, which offers a simplified representation while acknowledging the coupling between stator and rotor variables. This chapter sets the foundation for subsequent chapters, where advanced control techniques are introduced to overcome the challenges associated with motor control.

The second chapter emphasized the advantages of FOC over traditional scalar control methods. FOC enables precise control over current, speed, and torque, resulting in improved performance and energy efficiency. It achieves better current control with reduced harmonics and smoother operation. The speed regulation is enhanced, leading to improved tracking of reference speed and system dynamics. Additionally, FOC optimizes torque production, increasing torque density and overall motor efficiency.

The third chapter introduced the concept of stability in the sense of Lyapunov and presented the Backstepping control technique as a systematic approach for synthesizing control laws and ensuring stability. The application of Backstepping control to the induction motor demonstrated its effectiveness in stabilizing the machine, particularly during transient stages and varying load conditions. The results indicated that Backstepping control outperformed classical control techniques, highlighting its superior performance and robustness.

Overall, this thesis concludes that the combination of the Park model, FOC, and Backstepping control offers a comprehensive approach for induction motor control, providing improved performance, energy efficiency, and stability. These techniques can be advantageous for various applications involving induction motors..

BIBLIOGRAPHY

[1] Kim, S. H. (2017). Electric motor control: DC, AC, and BLDC motors. Elsevier.

[2] J. Pierre, P. Hautier et J. Faucher, « Modélisation et Commande de la machine asynchrone» Edition Technib, Paris, Octobre. 1995.

[3] F. Blaschke, “The Principle of Field Orientation as Applied to the NEW Transvector Closed-Loop System for Rotating-Field Machines,” Siemens Review, Vol. 34, No. 3, 1972, pp. 217-220

[4] Trabelsi, Ramzi, et al. "Backstepping control for an induction motor using an adaptive sliding rotor-flux observer." *Electric Power Systems Research* 93 (2012): 1-15.

[5] Boost, Michael A., and Phoivos D. Ziogas. "State-of-the-art carrier PWM techniques: a critical evaluation." IEEE transactions on industry applications 24.2 (1988): 271-280.

[6] Nait, M, S « Contribution à la commande vectorielle d’une machine asynchrone à cage d’écureuil : Robustesse Contre les Dérives Paramétrique, Amélioration des Performances énergétiques », Thèse de doctorat d’état, université de Batna 1999.

[7] W. Leonhard, «Control of AC-Machines with the help of Microelectronics,» 3rd IFAC Symposium on Control in Power Electronics and Electrical Drives, vol. 16, n° 16, pp. 769-792, 12-14 September 1983

[8] Lee, Kibok, Sara Ahmed, and Srdjan M. Lukic. "Universal restart strategy for scalar (V/f) controlled induction machines." *IEEE Transactions on Industry Applications* 53.6 (2017): 5489-5495.

[9] Khalil, Hassan K. "Nonlinear systems third edition." *Patience Hall* 115 (2002).

[10] B. Houssini, «Prototypage rapide a base de FPGA d’un algorithme de contrôle avancé le moteur a induction», Université du Québec, 2010.

[11] Horacio Márquez - Nonlinear Control Systems_ Analysis and Design (2003, Wiley-Interscience)

Notations and Symbols

S, R	Indices corresponding to the stator and the rotor
A, B et C	Indices corresponding to the three phases A, B and C
θ_{obs}	Angled observation of the PARK matrix
θ_r	Rotor electrical angle
θ_s	Stator electrical angle
V	Voltage
I	Current
R_S	Stator resistance
R_R	Rotor resistance
l_S	Stator self-inductance
l_R	Rotor self-inductance
L_S, L_R	Stator and rotor cycle inductance per phase
m_S, m_R	Coefficient of mutual inductance between two phases of the stator and rotor
m_{SR}	Maximum mutual inductance between a stator phase and a rotor phase
M	Cyclic mutual inductance
T_e	Electromagnetic torque.
T_l	Load torque
J	Moment of Inertia of the Rotating Part
f	Viscous coefficient of friction
Ω	mechanical speed
P	Number of pole pairs
T_S, T_R	Stator and rotor time constant
σ	Blondell's dispersion coefficient
$(\alpha \quad \beta)$	Axes corresponding to the frame of reference linked to the stator.
$(d \quad q)$	Axes corresponding to the reference frame linked to the rotating field
$(u \quad v)$	Two-phase system axes
G	Observer Gain
S	Operator derived from LAPLACE
$[p]$	PARK matrix
$[L_{ss}]$	Matrix of stator inductors
$[L_{RR}]$	Rotor inductors matrix
$[L_{sR}]$	Matrix of the mutual inductances of the stator rotor coupling.

Φ_{ref}	Reference flux
Ω_{ref}	Reference speed
$[A]$	System State Evolution Matrix
$[B]$	Control System Matrix
$[U]$	Order Matrix
Kp, Ki	Proportionality and Integration Coeffi
T_i	Time constant

ANNEX

The parameters of the machine used

Nameplate

V=220 / 380V

F= 50Hz

P = 2

Electrical parameters

R_s=4.85Ω

R_r=3.805Ω

L_s=0.274H

L_r=0.274H

M=0.258H

Mechanical Parameters

J=0.031 kgm2

F=0.008 S

Sample time

T_s=0.3e^{-6}

Reference speed

T (s)	0	1	4	6	8	10	12	14	16
Speed (rad/s)	0	50	50	100	100	0	0	25	25

Applied load torque

T (s)	0	2	2.01	3	3.01	7	7.01	16
Load torque (N.m)	0	0	10	10	0	0	10	10